New Phytologist

Research

A small cysteine-rich protein from two kingdoms of microbes is recognized as a novel pathogen-associated molecular pattern

Jiajun Nie, Zhiyuan Yin, Zhengpeng Li, Yuxing Wu and Lili Huang

State Key Laboratory of Crop Stress Biology for Arid Areas, College of Plant Protection, Northwest A&F University, Yangling, Shaanxi 712100, China

Author for correspondence:
Lili Huang
Tel: +86 29 8709 1312
Email: huanglili@nwsuaf.edu.cn

Received: *18 August 2018*
Accepted: *1 December 2018*

New Phytologist (2019) **222:** 995–1011
doi: 10.1111/nph.15631

Key words: cell death, filamentous pathogens, innate immunity, *Nicotiana benthamiana*, pathogen-associated molecular pattern (PAMP), *Valsa mali*.

Summary

- Pathogen-associated molecular patterns (PAMPs) are conserved molecules that are crucial for normal life cycle of microorganisms. However, the diversity of microbial PAMPs is little known. During screening of cell-death-inducing factors from the necrotrophic fungus *Valsa mali*, we identified a novel PAMP VmE02 that is widely spread in oomycetes and fungi.
- *Agrobacterium tumefaciens*-mediated transient expression or infiltration of recombinant protein produced by *Escherichia coli* was performed to assay elicitor activity of the proteins tested. Virus-induced gene silencing in *Nicotiana benthamiana* was used to determine the components involved in VmE02-triggered cell death. The role of VmE02 in virulence and conidiation of *V. mali* were characterized by gene deletion and complementation.
- We found that VmE02, together with some of its homologues from both oomycete and fungal species, exhibited cell-death-inducing activity in *N. benthamiana*. VmE02-triggered cell death was shown to be dependent on BRI1-ASSOCIATED KINASE-1, SUPPRESSOR OF BIR1-1, HSP90 and SGT1 in *N. benthamiana*. Deletion of *VmE02* in *V. mali* greatly attenuated pathogen conidiation but not virulence, and treatment of *N. benthamiana* with VmE02 enhances plant resistance to *Sclerotinia sclerotiorum* and *Phytophthora capsici*.
- We conclude that VmE02 is a novel cross-kingdom PAMP produced by several fungi and oomycetes.

Introduction

Filamentous fungi and oomycetes are among the most devastating plant pathogens in agriculture. During the continuous arms race of co-evolution between phytopathogens and their hosts, plants have shaped a multifaceted immune system. One of the important parts of defense is to perceive pathogen-associated molecular patterns (PAMPs) or microbe-associated molecular patterns by host receptors, leading to effective resistance responses that provide PAMP-triggered immunity (PTI) (Yu *et al.*, 2017).

PAMPs are evolutionarily conserved molecules that play essential roles in microbial fitness or survival (Medzhitov & Janeway, 1997; Nürnberger & Brunner, 2002; Thomma *et al.*, 2011). Flagellin, peptidoglycan and lipopolysaccharides are known as classical PAMPs in bacteria (Felix *et al.*, 1999; Dow *et al.*, 2000; Gust *et al.*, 2007); glucans and chitin are the best known PAMPs in oomycetes and fungi, respectively (Fliegmann *et al.*, 2004; Shinya *et al.*, 2015). In addition, the bacterial cold-shock proteins and proteinaceous eMAX, the fungal endopolygalacturonases (PGs) and xylanase EIX, along with the oomycete Pep13 and elicitin INF1 are also perceived as PAMPs by plants (Brunner *et al.*, 2002; Rotblat *et al.*, 2002; Felix & Boller, 2003; Jehle *et al.*, 2013; Zhang *et al.*, 2014; Du *et al.*, 2015). More recently, a proteinaceous PAMP that induces cell death in Solanaceae plants was identified in ascomycete fungi (Franco-Orozco *et al.*, 2017). Moreover, there are also PAMPs that are widely spread across microbial taxa, such as the necrosis and ethylene-inducing peptide 1-like proteins (NLPs), and the glycoside hydrolase 12 protein XEG1 (Qutob *et al.*, 2006; Oome *et al.*, 2014; Albert *et al.*, 2015; Ma *et al.*, 2015; Wang *et al.*, 2018). Both NLPs and XEG1 are extensively distributed in oomycetes, fungi, and bacteria. Regardless of this, we know remarkably little about the diversity of microbial PAMPs.

The leucine-rich repeat (LRR) receptor-like kinase (RLK) BRI1-ASSOCIATED KINASE-1 (BAK1)/SOMATIC EMBRYOGENESIS RECEPTOR KINASE 3 (SERK3) plays a central regulatory role in plant immunity (Heese *et al.*, 2007; Yasuda *et al.*, 2017). BAK1 regularly acts as a co-receptor by forming complexes with pattern-recognition receptors (PRRs), which is pivotal for immune signaling following PAMP recognition. For example, the *Arabidopsis* RLK FLAGELLIN-SENSING-2 (FLS2) binds the flagellin epitope flg22 and recruits BAK1 to form an active receptor complex (Chinchilla *et al.*, 2007; Heese *et al.*, 2007; Liebrand *et al.*, 2014); the receptor-like protein (RLP) ELR, which is responsible for INF1 recognition, associates with BAK1 to form a bipartite equivalent and activate defense responses in potato (Du *et al.*, 2015). Another well-characterized LRR-RLK involved in plant immunity and PAMP recognition is SUPPRESSOR OF BIR1-1 (SOBIR1) (Liebrand *et al.*, 2013,

2014; Liang & Zhou, 2018). SOBIR1 generally functions as a common adaptor to associate with various RLPs, forming RLP-adaptor complexes to regulate downstream defense signaling (Gust & Felix, 2014). For instance, in tomato, SOBIR1 physically interacts with the RLPs Cf-4 and Ve1, the combinations of which are indispensable for host resistance against *Cladosporium fulvum*-secreted Avr4 and *Verticillium dahlia*-secreted Ave1, respectively (Liebrand *et al.*, 2013). Moreover, BAK1 and SOBIR1 associate with RLP23, an RLP receptor for nlp20 (a conserved peptide from NLPs), to form a tripartite complex and induce plant resistance (Albert *et al.*, 2015).

Apart from LRR-RLKs, R protein-mediated signaling components like HSP90, SGT1, EDS1 and NDR1 may also be involved in PTI responses. It has been reported that, in addition to BAK1 and SOBIR1, both HSP90 and SGT1 are crucial for the *Phytophthora infestans* PAMP INF1-mediated hypersensitive response (HR) in *Nicotiana benthamiana* (Peart *et al.*, 2002; Kanzaki *et al.*, 2003; Heese *et al.*, 2007; Wang *et al.*, 2018). Similarly, an NLP from *P. infestans* also requires HSP90 and SGT1 for induction of plant cell death (Kanneganti *et al.*, 2006). Furthermore, as an RLP receptor for perceiving Ave1 (also known as a PAMP), Ve1 in tomato is dependent on both EDS1 and NDR1 for downstream signaling cascade (Fradin *et al.*, 2009; Liebrand *et al.*, 2013). In spite of this, the detailed mechanisms allowing plants to perceive PAMPs and active innate immunity remain largely elusive.

Valsa mali, the causal agent of apple *Valsa* canker, is a necrotrophic fungus that causes severe necrosis on apple trees, resulting in substantial yield losses in eastern Asia each year (Ke *et al.*, 2013; Li *et al.*, 2013). To date, molecular mechanisms of the virulence of *V. mali* remain obscure. Genome sequence of *V. mali* has been obtained (Yin *et al.*, 2015), greatly facilitating the exploration of pathogen virulence factors. Since necrotrophic pathogens infect and colonize host plants by cell killing, our original aim of this study is to characterize cell-death-inducing molecules from predicted candidate effector proteins (CEPs) of *V. mali*.

Here, in this study, we identified a small cysteine-rich protein, VmE02, that could induce cell death in various plants. We showed that VmE02 is widely conserved across oomycete and fungal pathogens, whose homologues of VmE02 can also trigger cell death in *N. benthamiana*. Additionally, we showed that VmE02 activates innate immunity in *N. benthamiana*, and its activation of cell death is dependent on BAK1, SOBIR1, HSP90 and SGT1. Moreover, VmE02 is important for conidiation of *V. mali*, and treatment of *N. benthamiana* with VmE02 enhances plant resistance to both fungal and oomycete pathogens. Collectively, this study revealed a novel cross-kingdom PAMP that is present in several fungal and oomycete species.

Materials and Methods

Strains and the growth of plants

The *V. mali* wild-type strain 03-8 and *V. mali* transformants were grown and maintained on potato dextrose agar medium at 25°C in the dark. *Escherichia coli* strain JM109 was used for plasmid construction, cultured on lysogeny broth medium at 37°C. The *Agrobacterium tumefaciens* strain GV3101 was used for agroinfiltration of plants, cultured on lysogeny broth medium at 28°C. *N. benthamiana*, *Solanum lycopersicum*, *Capsicum annuum* and *Arabidopsis thaliana* seedlings were grown in a glasshouse at 14 h 22°C : 10 h 20°C, day : night, 72% relative humidity.

Plasmid construction

V. mali candidate effector VM1G_04692 with signal peptide (SP) was amplified from *V. mali* complementary DNA (cDNA) library with gene-specific primers (Supporting Information Table S1) using Phusion High-Fidelity DNA Polymerase (New England Biolabs, Ipswich, MA, USA). Homologous genes of *VmE02* in *Puccinia striiformis* f. sp. *tritici* (*Pst*), *Phytophthora parasitica* and *Aspergillus nidulans* were amplified from corresponding pathogen cDNA libraries; homologous sequences in *Sclerotinia sclerotiorum* and *Botrytis cinerea* were amplified from synthetic double-strand DNAs produced by GENEWIZ, Inc. (Jiangsu, China). The amplicons were subsequently ligated with potato virus X (PVX) vector and PVX-*GFP* vector (pGR106, Wagner *et al.*, 2004) digested with specific enzymes (*Cla*I and *Sal*I for PVX vector, *Cla*I and *Sma*I for PVX-*GFP* vector), using ClonExpress II One-Step Cloning Kit (Vazyme, Nanjing, China). The SP(VmE02)-INF1$^{\Delta SP}$, SP(PR1)-GFP, and SP (VmE02)-GFP expression constructs were generated using ClonExpress MultiS One-Step Cloning Kit (Vazyme). For generation of *VmE02* gene-complementation constructs, PVX-*VmE02* vector was used as template to amplify the sequence, and the fragments were then ligated to pDL2-*GFP* vector (Zhou *et al.*, 2011) digested with *Xho*I. To create constructs for confocal microscopy, gene fragments amplified from PVX-*VmE02* vector were ligated to pCAMBIA1302-*GFP* (GenBank AF234298; Hajdukiewicz *et al.*, 1994) digested with *Spe*I and *Nco*I. Constructs used for virus-induced gene silencing (VIGS) in *N. benthamiana* were generated in the TRV2 vector (Liu *et al.*, 2002), using *N. benthamiana* cDNA library for gene fragment amplification. All constructs were validated by sequencing in Sangon (Sangon Biotech, Shanghai, China).

A. tumefaciens infiltration and trypan blue staining

The constructs were transformed into *A. tumefaciens* strain GV3101 using electroporation. After selection with selective antibiotics, individual colonies verified by PCR were cultured in lysogeny broth medium at 28°C in a shaking incubator at 220 rpm for 48 h. The bacteria were then pelleted by centrifugation and resuspended in MES buffer (10 mM magnesium chloride ($MgCl_2$), 10 mM MES, 200 μM acetosyringone, pH 5.7) in the dark for 3 h at room temperature (RT) before infiltration. For infiltration, suspended *A. tumefaciens* cells were mixed with P19 silencing suppressor (Voinnet *et al.*, 2003) and adjusted to a final OD_{600} of 0.6. *A. tumefaciens* cell suspension was infiltrated into plant leaves using a syringe without a needle. To determine cell-death-inducing activity of the proteins, PVX-*GFP* and PVX

constructs were agroinfiltrated into plants. Symptom development was monitored visually 3–5 d post agroinfiltration (dpa) for *N. benthamiana*, 10–15 dpa for *S. lycopersicum*, and 7–10 dpa for *C. annuum* leaves. Cell death symptom elicited by VmE02 recombinant protein was monitored 2–4 d post infiltration for *N. benthamiana*, *S. lycopersicum*, *Arabidopsis*, apple and wheat. Trypan blue staining was performed as described (Qi *et al.*, 2016). The experiments were repeated at least three times, and each assay consisted of at least three plant seedlings or leaves.

Measurement of electrolyte leakage

Ion leakage from leaf disks was measured to assay cell death as described (Yu *et al.*, 2012). Six leaf disks (1 cm diameter) from agroinfiltrated areas were taken and floated in 5 ml distilled water for 5 h, and the conductivity of bathing solution was measured using a conductivity meter (FE32 FiveEasy; Mettler-Toledo, Shanghai, China) to yield 'value A'. Then the leaf disks were boiled in the bathing solution in sealed tubes for 20 min. When the solution cooled to RT, the conductivity was measured to gain 'value B'. Ion leakage was calculated as percent leakage; that is, (value A/value B) × 100. Assays were repeated three times.

Expression and purification of VmE02

VmE02 without SP was amplified and cloned into *Nde*I and *Bam*HI sites of pET28a vector (Novagen Inc., Madison, WI, USA). VmE02 recombinant protein was expressed in *E. coli* strain BL21(DE3) cells. Expression was induced by adding 0.3 mM isopropyl-β-D-thiogalactopyrandoside for 24 h at 16°C. Cells were collected by centrifugation at 5000 ***g*** for 10 min. For protein extraction, cells were resuspended in lysis buffer (20 mM sodium hydrogen phosphate, 300 mM sodium chloride (NaCl), pH 7.4) plus 1 mg ml^{-1} lysozyme, 1 mM phenylmethanesulfonyl fluoride (PMSF), and 1.98 mM β-mercaptoethanol, followed by sonication and centrifugation at 10 000 ***g*** for 10 min. VmE02 was purified by affinity chromatography using Ni-NTA resin (Thermo Scientific, Waltham, MA, USA) following the manufacturer's instructions.

Apoplastic fluid extraction and confocal microscopy

The apoplastic fluid from *N. benthamiana* leaves was extracted by the infiltration-centrifugation method as described (O'Leary *et al.*, 2014). For confocal microscopy, *N. benthamiana* leaves were harvested 2 dpa and imaged using a confocal laser scanning microscope (Olympus microscope FV1000, Tokyo, Japan). Green fluorescent protein (GFP) fluorescence was captured using an excitation wavelength of 488 nm and an emission wavelength of 505–530 nm. The fluorescence of mCherry was excited with a 559 nm wavelength laser to detecte specific emissions between 600 and 680 nm. The TaWPI6 protein from wheat (Imai *et al.*, 2005) was used as a marker for plasma membrane. For fluorescence detection after plasmolysis, *N. benthamiana* leaves were exposed to 1.5 M NaCl for 5 min before observation. Confocal microscopy was performed at least twice.

RNA isolation and quantitative reverse transcription PCR analysis

Total RNA was isolated using Quick RNA isolation Kit (Huayueyang, Beijing, China) according to the manufacturer's protocol and was quantified using a NanoDrop Micro Photopeter (NanoDrop, Wilmington, DE, USA). First-strand cDNA was synthesized from 1 μg of total RNA, using the RevertAid First Strand cDNA Synthesis Kit (Thermo Scientific), followed by quantitative reverse transcription-PCR (qRT-PCR) using RealStar Green Mixture (GenStar, Beijing, China). qRT-PCR was performed with a CFX Connect Real-Time System (Bio-Rad, Hercules, CA, USA). The *G6PDH* gene in *V. mali* (Yin *et al.*, 2013) and *NbActin* in *N. benthamiana* (Sainsbury & Lomonossoff, 2008) were used as internal controls to normalize the gene expression. Relative expression levels were determined using the $2^{-\Delta\Delta CT}$ method with three independent biological replicates (Livak & Schmittgen, 2001).

Yeast signal sequence trap

Functional validation of the predicted SP was conducted with a yeast secretion system (Jacobs *et al.*, 1997). DNA fragments encoding SP of VmE02 were amplified using specific primers (Table S1) and introduced into pSUC2 to create in-frame fusion with the invertase. The pSUC2-$VmE02^{SP}$ vector was transformed into the yeast strain YTK12 and screened on CMD-W (lacking tryptophan) medium. Positive colonies were replica-plated on YPRAA medium plates for invertase secretion. YTK12 transformed with pSUC2-$Avr1b^{SP}$ and the empty pSUC2 vector was used as a positive and negative control, respectively.

Transformants generation and virulence tests

For generation of *VmE02* deletion mutants in *V. mali*, transformed *V. mali* lines were obtained using polyethylene glycol (PEG)-mediated protoplast transformation (Gao *et al.*, 2011), according to a method described previously (Fig. S1; Li *et al.*, 2015). Positive transformants were screened using genomic PCR with the primers listed in Table S1, which were further confirmed by Southern blotting using the DIG DNA Labeling and Detection Kit II (Roche, Mannheim, Germany) according to the manufacturer's instructions. To obtain *VmE02* complementation transformants, pDL2-*GFP* construct was introduced into *VmE02* deletion mutants, using PEG-mediated protoplast transformation.

For *V. mali* virulence and conidiation tests, detached apple twigs from *Malus domestica* Borkh. cv Fuji were inoculated with wild-type strain 03-8, *VmE02* deletion mutants, or *VmE02* complementation transformants as described (Wei *et al.*, 2010). For infection by *S. sclerotiorum* and *P. capsici* in *N. benthamiana*, 24 h after infiltration of purified VmE02 recombinant protein, fresh mycelial plugs with 5 mm diameters were inoculated on the center of *N. benthamiana* leaves. Inoculated plants were put in a transparent box to keep high humidity. The lesion diameters caused by *S. sclerotiorum* were calculated 24 h post-inoculation

(hpi). Disease progression of *P. capsici* was evaluated 60 hpi by quantification of relative biomass using qRT-PCR as described (Yu *et al.*, 2012). Assays were repeated at least three times, and each assay was performed with three independent biological replicates.

VIGS in *N. benthamiana*

For tobacco rattle virus (TRV)-mediated gene silencing assays, *A. tumefaciens* strain GV3101 was transformed with TRV1, and TRV2 constructs by electroporation. *A. tumefaciens* cultures expressing TRV2 constructs were mixed with *A. tumefaciens* culture expressing TRV1 in a 1 : 1 ratio in MES buffer (10 mM $MgCl_2$, 10 mM MES, 200 μM acetosyringone, pH 5.7), to a final OD_{600} of 0.8. After standing at RT for 3 h, the mixed culture was injected into two or three primary leaves of four-leaf-stage *N. benthamiana* seedlings. pTRV2:*PDS* and TRV:*GFP* were used as controls. At 3 wk after agroinfiltration of TRV2 constructs, plants were agroinfiltrated with VmE02 or INF1. The experiments were repeated three times, and each assay consisted of at least six plants with three inoculated leaves. The efficiency of gene silencing was validated by qRT-PCR analysis.

Sodium dodecyl sulfate polyacrylamide gel electrophoresis and Western blotting

Protein samples from agroinfiltrated plants (or protein samples from *V. mali* mycelia) were prepared using lysis buffer (50 mM Tris (pH7.5), 150 mM NaCl, 1 mM EDTA, 1% TritonX-100, 1% sodium deoxycholate) plus 1 mM PMSF and 1% proteinase inhibitor cocktail (Sigma-Aldrich) by grinding 400 mg of leaf tissue (or 100 mg mycelia) in 400 μl lysis buffer. The total protein was centrifuged at 4°C for 10 min at 14 549 ***g*** and the supernatant was then transferred to a new tube. The samples were boiled for 10 min in ×2 sodium dodecyl sulfate (SDS) loading buffer and then loaded on a gel for SDS polyacrylamide gel electrophoresis.

After electrophoresis, proteins were transferred from the gel to a polyvinylidene difluoride membrane using a transfer buffer (20 mM Tris, 150 mM glycine). The membrane was rinsed in Tris buffered saline (TBS) and then blocked in 5% nonfat dry milk in TBST (TBS with 0.1% Tween 20) for 2 h at RT with 50 rpm shaking, followed by incubation with the mouse anti-GFP or anti-His monoclonal antibody (Sungenebiotech, Tianjin, China) at 4°C overnight. After washing by TBST three times, the membrane was incubated with goat-anti mouse IgG (Cwbiotech, Beijing, China) secondary antibody at RT for 1 h. Protein bands were detected using ECL substrate (Solarbio, Beijing, China) following the manufacturer's instructions.

Bioinformatics analysis

Homologous sequences of VmE02 in different pathogens were obtained by querying VmE02 protein sequence against the NCBI database from the genome of corresponding species, using BLAST search programs (https://blast.ncbi.nlm.nih.gov/Blast.cgi), with a BLAST *E*-value cut-off of 1e-10. Sequence motifs were identified by the MEME Suite (Bailey *et al.*, 2009) with default settings, except the number of motifs was set at 8. The multiple sequence alignment of VmE02 and its homologues was generated using the MUSCLE algorithm (Edgar, 2004). The signal peptide was predicted using the SIGNALP 4.1 server (http://www.cbs.dtu.dk/services/SignalP/). Phylogenetic dendrograms were constructed using MEGA7 with maximum likelihood (Kumar *et al.*, 2016). The phylogenetic tree was viewed by EVOLVIEW (He *et al.*, 2016). The diagrams of protein sequences in this study were illustrated by IBS (Liu *et al.*, 2015).

Accession numbers

Sequence data from this article can be found in the GenBank/EMBL data libraries under the following accession nos. VmE02 (KUI69068.1), PPTG_02039 (XP_008893679.1), PPTG_14297 (XP_008909123.1), PPTG_09966 (XP_008904024.1), AN6672.2 (XP_664276.1), sscle_06g048920 (APA10122.1), SS1G_07491 (XP_001592044), BC1G_05134 (XP_001555760), PSTG_00149 (KNF06837.1), PSTG_13167 (KNE93445.1), and PSTG_16598 (KNE89953.1).

Results

VmE02 is an elicitor of plant cell death

A total of 193 CEPs were predicted to be encoded by the *V. mali* genome (Li *et al.*, 2015). With the aim to identify cell-death-inducing factors of *V. mali*, we carried out transient expression of these CEPs in *N. benthamiana*. The coding sequences of 50 randomly selected CEPs (Table S2) were cloned into PVX vectors, followed by agroinfiltration in *N. benthamiana*, with *GFP* and *Bax* used as negative and positive controls, respectively. It was shown that, 5 dpa, a protein of unknown function, VM1G_04692 (hereafter designated VmE02), induced intense cell death in *N. benthamiana* (Fig. 1a–c). By contrast, GFP control did not induce plant cell death, suggesting the cell death was specifically activated by VmE02.

To examine the specificity of plant response to VmE02, we agroinfiltrated VmE02 into expanded leaves of tomato (*S. lycopersicum*) and pepper (*C. annuum*). The result indicated that VmE02 also triggered cell death in the two plants tested (Fig. 1d–g). To further test the host range of VmE02, the recombinant protein was produced in *E. coli* (Fig. S2a,b). It showed that purified VmE02 recombinant protein retained cell-death-inducing activity (Fig. S2c,d), and it could also induce cell death in *Arabidopsis* (*A. thaliana*), its cognate host, and apple, but not in the monocot wheat (Fig. 1h–j). These results suggest that VmE02 can elicit cell death in multiple plant species.

VmE02 is a small cysteine-rich protein that requires apoplastic location for full cell-death-inducing activity

VmE02 contains 146 amino acids (aa), including 10 cysteine residues, which account for 6.8% of the full protein sequence

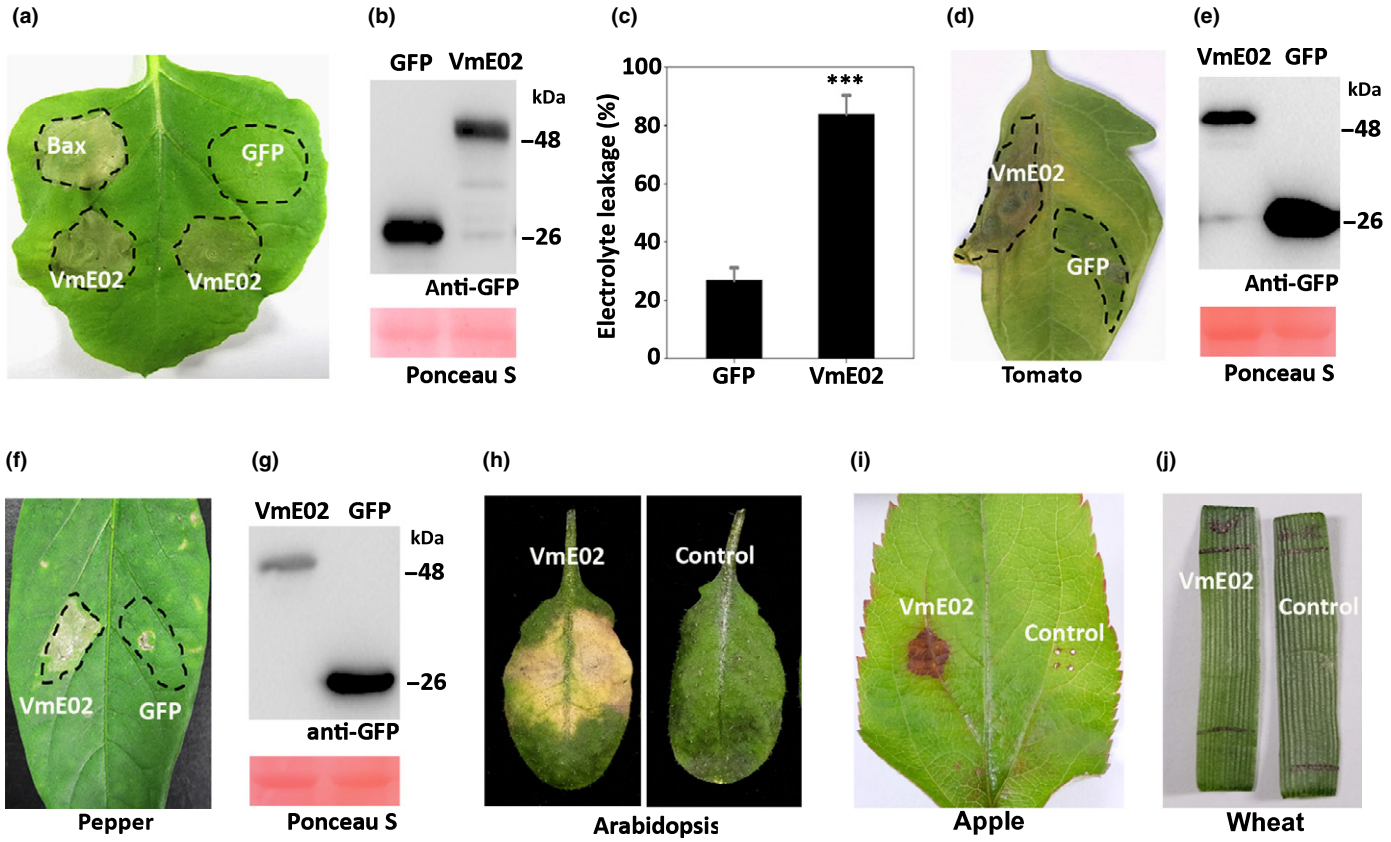

Fig. 1 VmE02 induces cell death in multiple plant species. (a) VmE02-induced cell death in *Nicotiana benthamiana*. Leaves of *N. benthamiana* were infiltrated with *Agrobacterium tumefaciens* carrying potato virus X (PVX)-*VmE02-GFP*, PVX-*Bax*, or PVX-*GFP*. Photographs were taken 5 d post agroinfiltration (dpa). (b) Immunoblot analysis of proteins in *N. benthamiana* transiently expressing green fluorescent protein (GFP) control and VmE02 fused with GFP tag. (c) Quantification of cell death by measuring electrolyte leakage. Means and SEs were calculated from three independent experiments. The statistical analyses were performed with Student's *t*-test. Bars indicate ± SE. ***, $P < 0.001$. (d, f) Cell death response in tomato and pepper triggered by VmE02. Leaves of tomato and pepper were infiltrated with *A. tumefaciens* carrying PVX-*VmE02-GFP* (on the left half) or PVX-*GFP* (on the right half). Photographs were taken 15 dpa for tomato and 10 dpa for pepper. (e, g) Immunoblot analysis of proteins in tomato (e) and pepper (g) transiently expressing GFP control and VmE02 fused with GFP tag. (h, i, j) Cell death response in *Arabidopsis*, apple and wheat triggered by 20 μM purified VmE02 recombinant protein or buffer control. VmE02 protein was infiltrated in *Arabidopsis* and wheat or dropped on the needle-pricked area of apple leaves. Photographs were taken 4 d post treatment (dpt) for *Arabidopsis* and wheat and 2 dpt for apple.

(Fig. S3a). Bioinformatics analysis indicated that VmE02 has a predicted N-terminal SP (1–18 aa) (Fig. S3a), suggesting it may be a secreted protein. Using a signal sequence trap system (Jacobs *et al.*, 1997), the SP of VmE02 was shown to be sufficient for the secretion of invertase in yeast (Fig. S3b). In addition, when the SP of INF1 elicitin was substituted by that of VmE02, the fusion protein could successfully induce cell death in *N. benthamiana* (Fig. S3c). Thus, the SP of VmE02 is functional and VmE02 is most likely to be secreted.

To test whether VmE02 needs to be targeted to apoplast to trigger plant cell death, VmE02 lacking SP (VmE02$^{\Delta SP}$) was transiently expressed in *N. benthamiana*. The results illustrated that VmE02$^{\Delta SP}$ greatly delayed cell death activation in *N. benthamiana* (Fig. 2a–e). *N. benthamiana* expressing full-length VmE02 began to show cell death symptom 3 dpa, whereas VmE02$^{\Delta SP}$ did not show cell death until 5 dpa. Furthermore, full-length VmE02 induced more intense cell death than VmE02$^{\Delta SP}$ did, which was confirmed by quantification of ion leakage (Fig. 2c,d). In contrast, a functional SP does not influence the GFP control in cell death activation (Fig. S4). These results indicate that the SP is important for the function of VmE02.

To validate the apoplastic location of full-length VmE02 targeted by its native SP, we agroinfiltrated pCAMBIA1302-*VmE02-GFP* and pCAMBIA1302-*VmE02*$^{\Delta SP}$*-GFP* vectors in *N. benthamiana* and used Western blotting to detect the GFP fusion proteins in apoplastic fluid of *N. benthamiana* leaves. It was shown that both VmE02-GFP and VmE02$^{\Delta SP}$-GFP can be detected in total protein samples (Fig. 2f). However, only VmE02-GFP could be successfully detected in apoplastic fluid (Fig. 2f), indicating the apoplastic location of full-length VmE02. Moreover, confocal microscopy revealed that VmE02-GFP, but not VmE02$^{\Delta SP}$-GFP, can be observed in apoplast of *N. benthamiana* cells after plasmolysis (Fig. S5), further confirming the extracellular location of VmE02. Taken together, these data indicate that extracellular space is essential for full cell-death-inducing activity of VmE02.

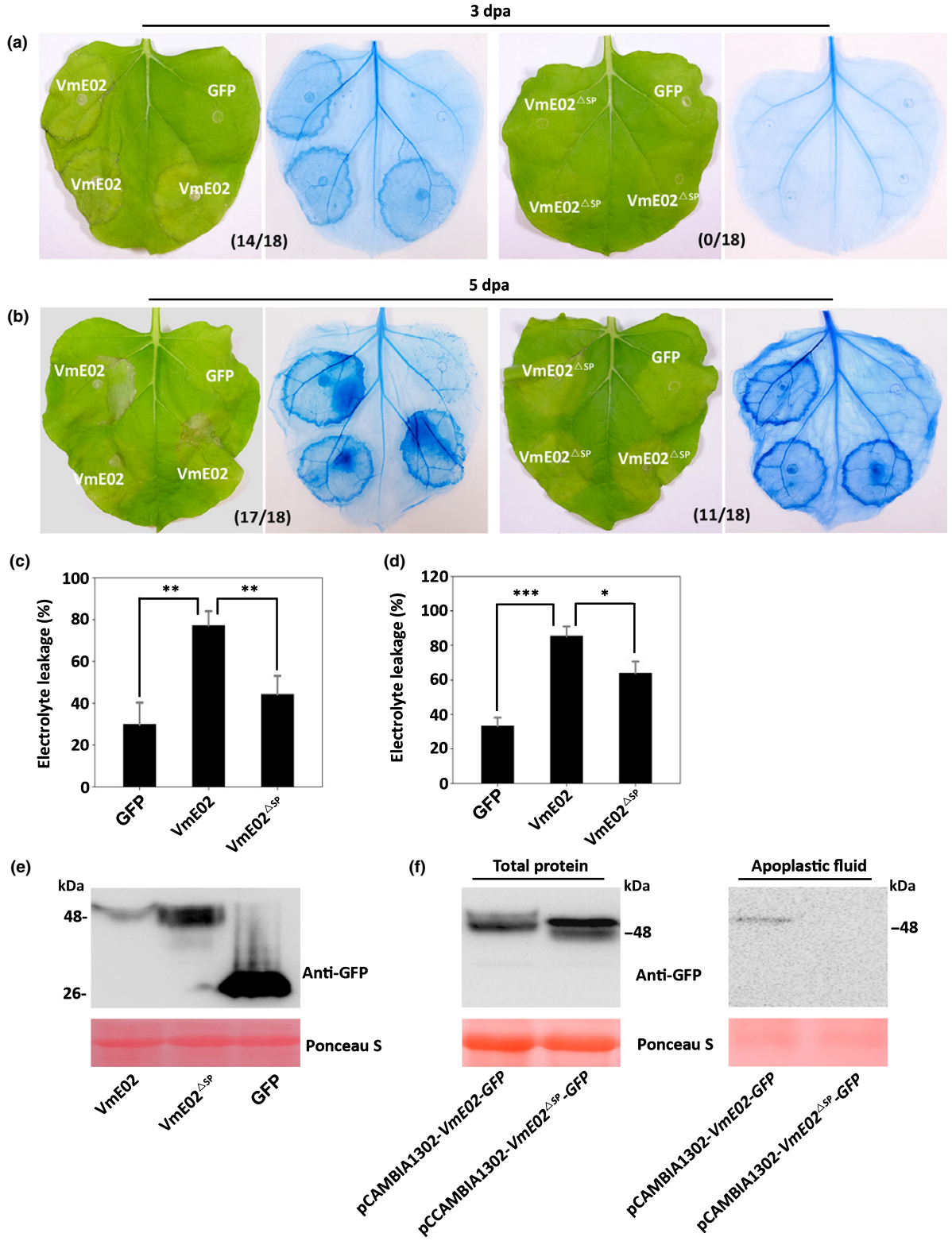

Fig. 2 Apoplastic location of VmE02 is required for full cell-death-inducing activity. (a, b) Cell death response in *Nicotiana benthamiana* expressing VmE02 and VmE02 lacking signal peptide (SP) (VmE02$^{\Delta SP}$). PVX-*VmE02-GFP* and PVX-*VmE02*$^{\Delta SP}$*-GFP* were agroinfiltrated into *N. benthamiana* leaves. Photographs were taken 3 d post agroinfiltration (dpa) (a) and 5 dpa (b). Cell death symptoms were further visualized by trypan blue staining. Ratios indicate the proportion of infiltrated sites that developed the cell death phenotype. (c, d) Quantification of cell death by measuring electrolyte leakage 3 and 5 dpa. Means and SEs were calculated from three independent experiments. The statistical analyses were performed with Student's *t*-test. Bars indicate ± SE. *, $P < 0.05$; **, $P < 0.01$; ***, $P < 0.001$. (e) Western blotting of proteins from *N. benthamiana* expressing green fluorescent protein (GFP) control, VmE02 and VmE02$^{\Delta SP}$ fused with GFP tag. (f) Western blotting analysis of apoplastic fluid and total proteins from *N. benthamiana* leaves agroinfiltrated with pCAMBIA1302-*VmE02-GFP* or pCAMBIA1302-*VmE02*$^{\Delta SP}$*-GFP*.

VmE02 is conserved in oomycetes and fungi, which contain VmE02 homologues that also induce cell death in *N. benthamiana*

To study the phylogenetic distribution of VmE02 homologues in different organisms, we queried the VmE02 protein sequence against the NCBI database from genomes of nine oomycetes, 29 fungi, five bacteria and five plants. This enabled identification of 67 homologous sequences in various oomycete and fungal species with diverse lifestyles (Fig. 3a). No homologues in plants or prokaryotic bacteria were identified, indicating evolutionary conservation of VmE02 among oomycete and fungal species (Fig. 3b). Searching for motifs by MEME within these sequences showed that there might be eight conserved motifs among them (Fig. S6), indicating a high level of sequence conservation for these proteins.

VmE02 is single-copied in *V. mali*, and most of the selected genomes contain no more than four homologues (Fig. 3b). Intriguingly, however, the number of VmE02 homologues in the biotrophic rust fungi, including *Pst*, *Puccinia graminis* f. sp. *tritici* and *Puccinia triticina*, is much larger than that of other species, with 10, 9 and 7, respectively (Fig. 3b). Our previous study reported that VmE02 was transferred from fungi to oomycetes via horizontal gene transfer (HGT; Yin *et al.*, 2016). Based on the phylogenetic analysis (Fig. 3a), VmE02 seems to be exclusively transferred from fungi to *Phytophthora* species, since no homologues were found in species of other genera such as *Pythium ultimum*, *Saprolegnia parasitica*, or *Peronospora parasitica* (Fig. 3b).

Given the sequence conservation of VmE02 in oomycetes and fungi, we tested whether VmE02 homologues could also trigger plant cell death. For this, *VmE02* homologous genes from

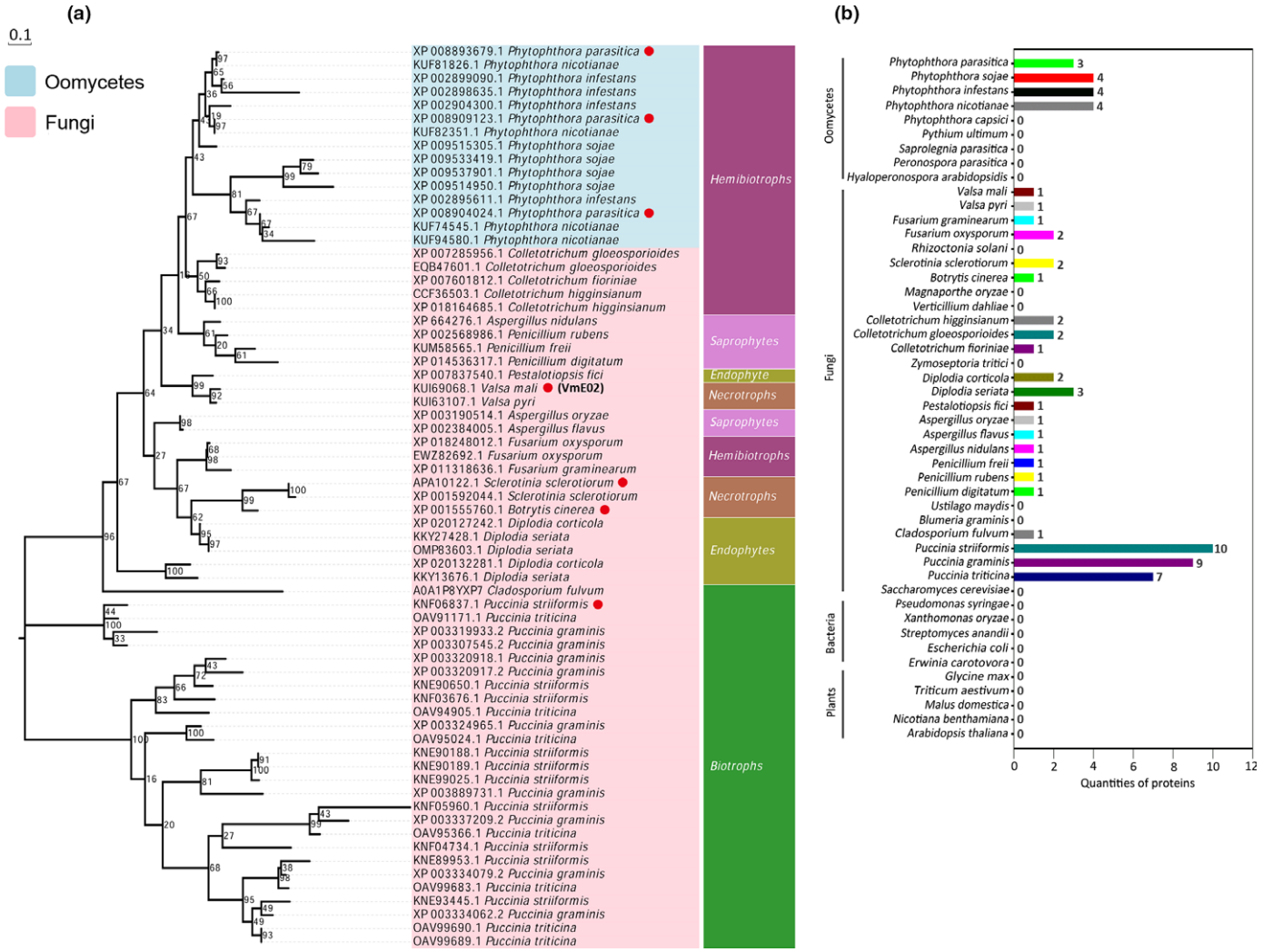

Fig. 3 VmE02 homologues are widely distributed across fungi and oomycetes. (a) The phylogeny of VmE02 and its homologous sequences from selected species. The tree was constructed with the maximum-likelihood method. Bootstrap percentage support for each branch is indicated. Sequences from oomycetes and fungi are marked with light blue and pink background, respectively. Colored stripes represent the lifestyles of corresponding species are present. The homologues shown to induce cell death in *Nicotiana benthamiana* are indicated by a red circle. (b) Distribution of VmE02 homologous proteins. The quantities of homologous sequences in selected species are indicated.

oomycetes and fungi, including the hemibiotrophic *Phytophthora parasitica*, the biotrophic *Pst*, the necrotrophic *S. sclerotiorum* and *B. cinerea*, together with the saprophytic *A. nidulans*, were cloned. Sequence analysis revealed that they are similar at sequence level, and they all contain an N-terminal SP (Fig. S7). When transiently expressed in *N. benthamiana*, PPTG_02039, PPTG_14297, and PPTG_09966 from *Phytophthora parasitica*, PSTG_00149 from *Pst*, sscle_06g048920 from *S. sclerotiorum*, and BC1G_05134 from *B. cinerea* also triggered cell death (Fig. 4a–c), suggesting a conserved function in cell death activation of these proteins. However, PSTG_13167 and PSTG_16598 from *Pst*, SS1G_07491 from *S. sclerotiorum*, and AN6672.2 from *A. nidulans* failed to trigger cell death (Fig. 4a–c). These data indicate homologues of VmE02 exist in both oomycetes and fungi, albeit with their divergent lifestyles, that are also capable of inducing cell death in *N. benthamiana*.

VmE02 triggers plant immunity responses

Plant cell death triggered by phytopathogen-derived molecules often arises from plant recognition and the subsequent defense responses known as HR (Coll *et al.*, 2011). To determine whether VmE02-activated cell death was associated with plant immunity responses, we examined reactive oxygen species (ROS) accumulation, callose deposition, together with the expression of two HR-specific marker genes, *HSR203J* and *HIN1* (Pontier *et al.*, 1994; Takahashi *et al.*, 2004), in *N. benthamiana*. It was shown that, 24 h after infiltration of 500 nM purified VmE02 protein in *N. benthamiana* leaves, enormous ROS accumulation and extensive callose deposition could be detected (Fig. 5a). In addition, the expressions of *NbHIN1* and *NbHSR203J* were greatly activated by VmE02 only 6 h post infiltration (Fig. 5b). These results suggest that VmE02 can be recognized by *N. benthamiana* and activate HR-associated immunity.

To clarify whether VmE02-activated immunity was accompanied with alteration of hormone signaling pathways, we further examined the transcript levels of well-known defense-related marker genes in *N. benthamiana*. These include: *NbPR1a* and *NbPR2*, marker genes of salicylic acid (SA)-dependent immunity (Dean *et al.*, 2005); *NbPR4* and *NbLOX*, marker genes of jasmonic acid (JA)-dependent immunity (Asai & Yoshioka, 2009;

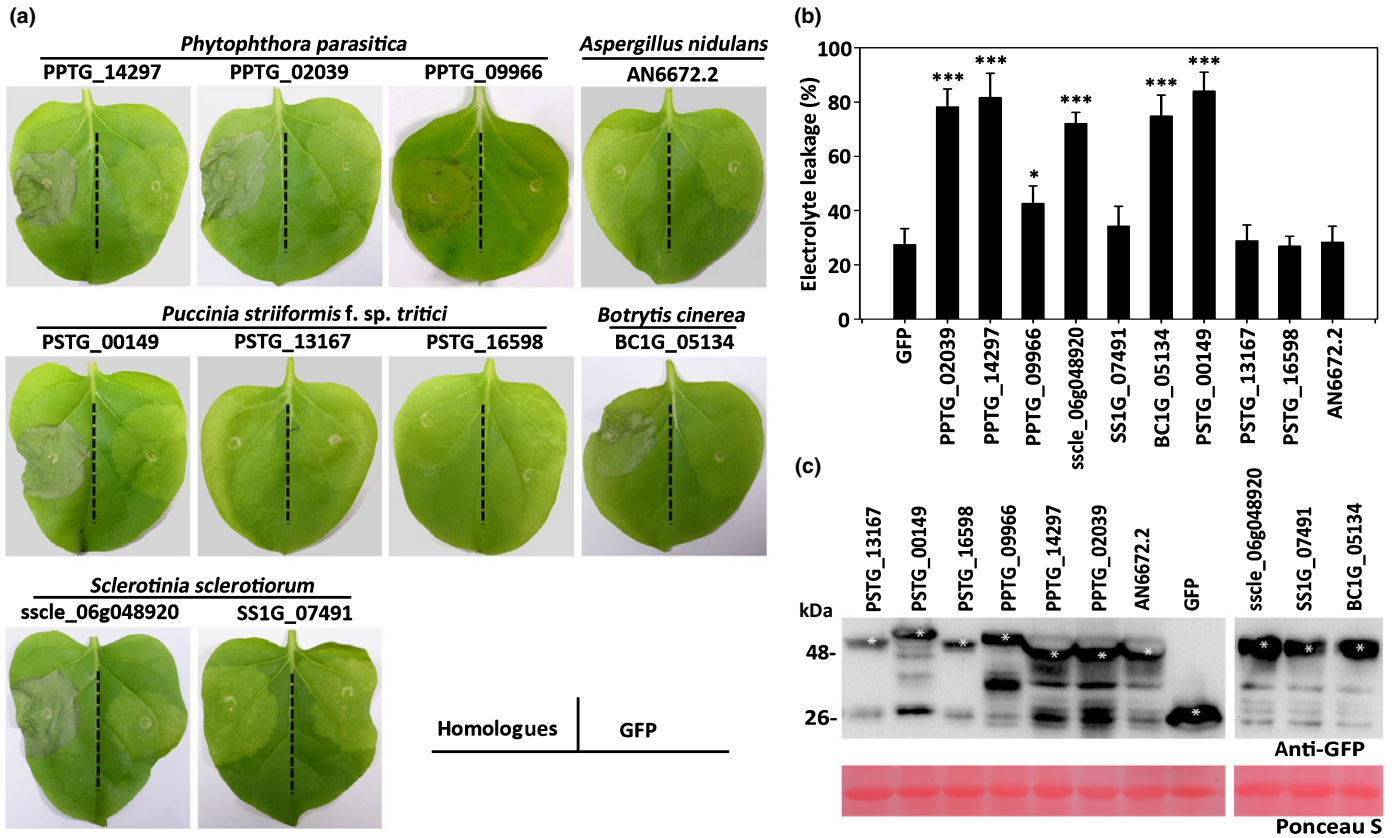

Fig. 4 VmE02 homologues from oomycete and fungal species elicit cell death in *Nicotiana benthamiana*. (a) Cell death response in *N. benthamiana* induced by VmE02 homologues. PPTG_02039, PPTG_14297 and PPTG_09966 from *Phytophthora parasitica*, AN6672.2 from *Aspergillus nidulans*, PSTG_00149, PSTG_13167 and PSTG_16598 from *Puccinia striiformis* f. sp. *tritici*, BC1G_05134 from *Botrytis cinerea*, and sscle_06g048920 and SS1G_07491 from *Sclerotinia sclerotiorum* were transiently expressed in *N. benthamiana* by infiltration of *Agrobacterium tumefaciens* carrying the potato virus X (PVX)-green fluorescent protein (*GFP*) constructs indicated. Photographs were taken 5 d post agroinfiltration. (b) Quantification of cell death by electrolyte leakage measurement. Means and SEs were calculated from three independent experiments. The statistical analyses were performed with Student's *t*-test. Bars indicate ± SE. *, $P < 0.05$; ***, $P < 0.001$. (c) Immunoblotting of proteins expressing corresponding homologues fused with GFP tag. White asterisks indicate the protein bands of interest.

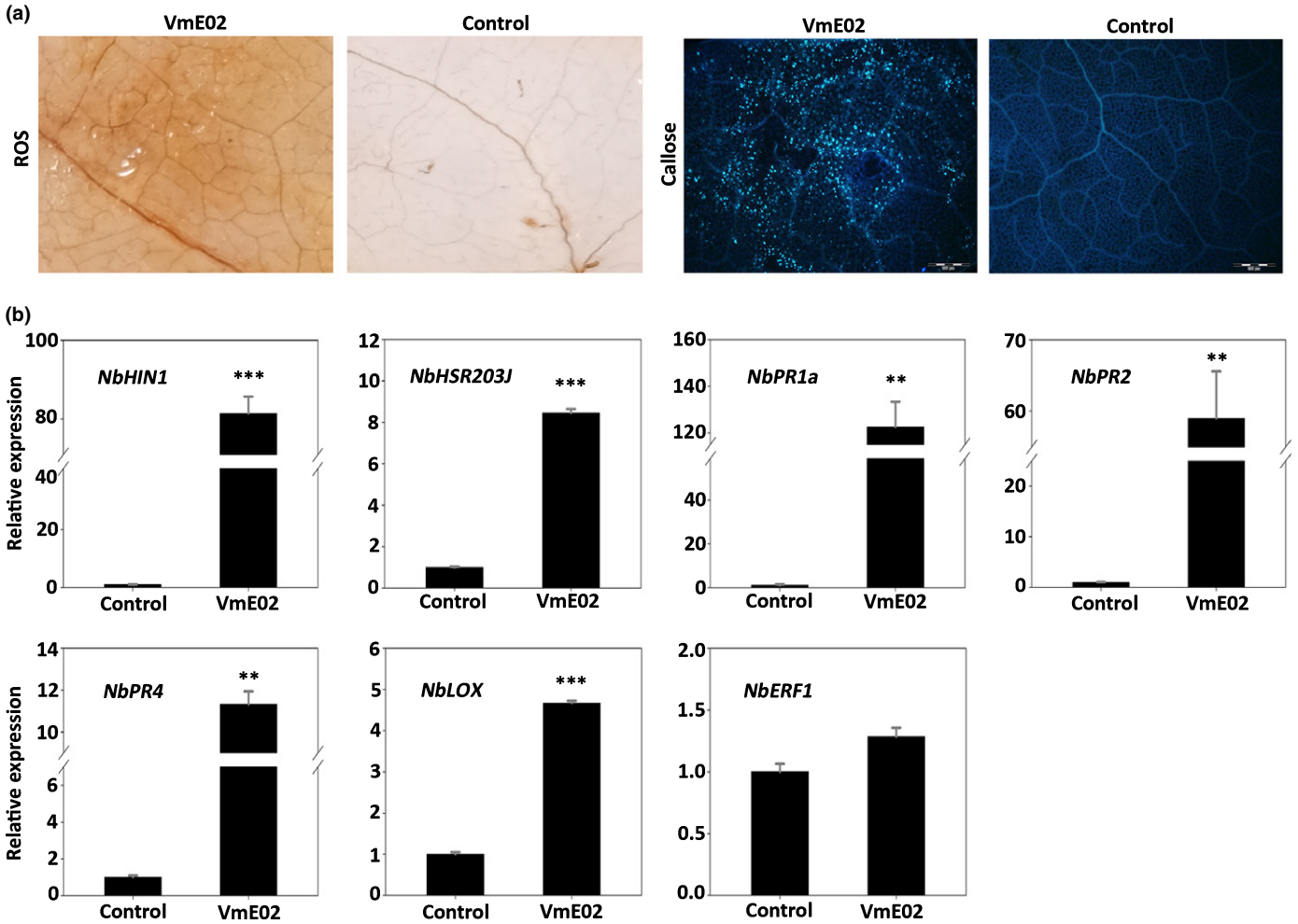

Fig. 5 VmE02 triggers plant immunity responses in *Nicotiana benthamiana*. (a) Accumulation of reactive oxygen species (ROS) and deposition of callose in *N. benthamiana*. *N. benthamiana* leaves were infiltrated with 500 nM purified VmE02 or buffer control for 24 h. For observation of callose, bars are 200 μm. (b) Relative expression of hypersensitive-response-specific marker genes and defense-related marker genes in *N. benthamiana*. *N. benthamiana* leaves were infiltrated with 500 nM purified VmE02 or buffer control for 6 h. Total RNA was extracted and transcript levels were monitored by quantitative reverse transcription PCR. *NbActin* was used as the internal reference gene. Relative expression of genes tested was normalized to *NbActin* and calibrated to the levels of buffer control (set as 1). Means and SEs were calculated from three biological replicates. The statistical analyses were performed with Student's *t*-test. Bars indicate ± SE. **, $P < 0.01$; ***, $P < 0.001$.

Rodriguez *et al.*, 2014); and *NbERF1*, one of the marker genes for ethylene-dependent immunity (Asai & Yoshioka, 2009; Pieterse *et al.*, 2012). As shown in Fig. 5(b), the transcripts of *NbPR1a*, *NbPR2*, *NbPR4* and *NbLOX* were considerably accumulated in *VmE02*-expressing samples, compared with the control. In contrast, there was no apparent change for the expression of *NbERF1* (Fig. 5b). Similar results were obtained in VmE02-treated apple leaves (Fig. S8). These findings demonstrate that VmE02 could trigger innate immunity by activation of SA- and JA-mediated defense pathways.

VmE02 induces the expression of PTI marker genes

The conservation of VmE02 in filamentous pathogens and its activation of plant immunity prompted us to speculate that VmE02 might serve as a microbial PAMP. To test this hypothesis, we first examined whether VmE02 promotes transcript accumulation of PTI marker genes. As shown in Fig. 6, the expression of PTI marker genes *NbCYP71D20* (Heese *et al.*, 2007), *NbPTI5*, *NbACRE31*, *NbWRKY7* and *NbWRKY8* (McLellan *et al.*, 2013) were dramatically activated in *N. benthamiana* by 500 nM VmE02, indicating VmE02 is likely to be a PAMP.

SERK3/BAK1, SOBIR1, HSP90 and SGT1 are required for VmE02-induced cell death in *N. benthamiana*

The receptor-associated kinases BAK1/SERK3 and SOBIR1 are essential regulatory components that facilitate intracellular signaling after perception of most PAMPs (Heese *et al.*, 2007; Liebrand *et al.*, 2013, 2014). To further determine whether VmE02 functions as a PAMP, we next tested whether BAK1 and SOBIR1 mediate VmE02-induced cell death in *N. benthamiana*. For this, VIGS constructs were generated to target *BAK1* and *SOBIR1*

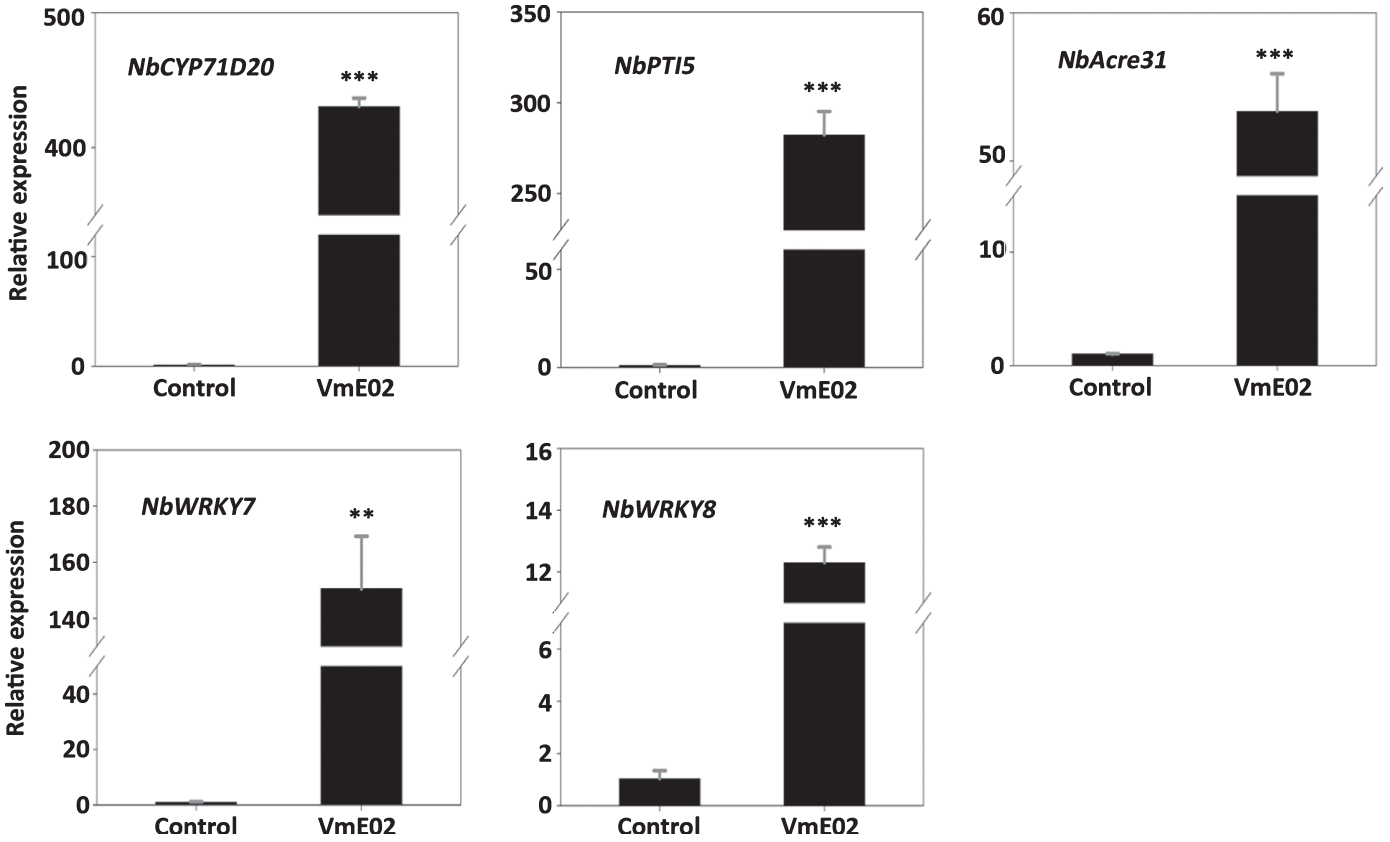

Fig. 6 VmE02 promotes transcript accumulation of pathogen-associated molecular pattern (PAMP)-triggered immunity (PTI) marker genes in *Nicotiana benthamiana*. *N. benthamiana* leaves were infiltrated with 500 nM purified VmE02 or buffer control. 6 h post infiltration, total RNA of *N. benthamiana* leaves was extracted. Relative expression levels of *NbCYP71D20*, *NbPTI5*, *NbACRE31*, *NbWRKY7* and *NbWRKY8* were analyzed by quantitative reverse transcription PCR. *NbActin* was used as the internal reference gene. Relative expression of tested genes was normalized to *NbActin* and calibrated to the levels of buffer control (set as 1). Means and SEs were calculated from three biological replicates. The statistical analyses were performed by Student's *t*-test. Bars indicate ± SE. **, $P < 0.01$; ***, $P < 0.001$.

expression in *N. benthamiana*. At 3 wk after agroinfiltration of TRV constructs, the plants were agroinfiltrated with VmE02 or INF1. The results showed that VmE02 failed to trigger cell death in both *BAK1*- and *SOBIR1*-silenced plants, as the positive control INF1 did (Fig. 7a,d,g). By contrast, VmE02 and INF1 still activated cell death in *N. benthamiana* plants treated with TRV2:*GFP* (Fig. 7a,d,g). Western bolting confirmed that VmE02 was successfully expressed in these silenced plants (Fig. 7b,e), and qRT-PCR analysis revealed that *BAK1* and *SOBIR1* expressions were considerably reduced in corresponding plants (Fig. 7c,f). Therefore, VmE02 is a PAMP dependent on BAK1 and SOBIR1 in *N. benthamiana*.

In order to gain more insights into the signaling components involved in VmE02-triggered cell death, we generated TRV constructs to knock down the expression of *HSP90*, *SGT1*, *EDS1* and *NDR1* in *N. benthamiana*. It was shown that, 3 wk following viral infiltration, cell death caused by VmE02 and INF1 was greatly compromised in *HSP90*- and *SGT1*-silenced plants, compared with *N. benthamiana* inoculated with TRV2:*GFP* (Fig. 7h–n). However, silencing of *EDS1* and *NDR1* showed no apparent influence on VmE02- and INF1-triggered cell death (Fig. S9). These results suggest that, apart from BAK1 and SOBIR1, VmE02 also requires HSP90 and SGT1, but not EDS1 or NDR1, for cell death activation in *N. benthamiana*.

Fig. 7 VmE02-triggered cell death in *Nicotiana benthamiana* requires BRI1-ASSOCIATED KINASE-1 (BAK1), SUPPRESSOR OF BIR1-1 (SOBIR1), HSP90 and SGT1. (a, d, h, k) Cell death response in *BAK1*-, *SOBIR1*-, *HSP90*- or *SGT1*-silenced *N. benthamiana* plants induced by VmE02 and INF1. *N. benthamiana* plants were subjected to virus-induced gene silencing (VIGS) by inoculation of tobacco rattle virus (TRV) constructs (TRV2:*GFP*, TRV2:*BAK1*, TRV2:*SOBIR1*, TRV2:*HSP90*, or TRV2:*SGT1*). At 3 wk after viral inoculation, *Agrobacterium tumefaciens* carrying the constructs indicated were infiltrated into gene-silenced *N. benthamiana* leaves. Photographs were taken 4 d post agroinfiltration. The experiment was performed three times with six plants for each TRV construct. Photographs of representative plant responses are shown. (b, e, i, l) Immunoblot analysis proteins from gene-silenced *N. benthamiana* leaves transiently expressing green fluorescent protein (GFP), and VmE02 fused with GFP tag. (c, f, j, m) *N. benthamiana BAK1*, *SOBIR1*, *HSP90* and *SGT1* expression levels after VIGS treatment determined by quantitative reverse transcription PCR analysis. *NbActin* was used as the internal reference gene. Means and SEs were calculated from three biological replicates. The statistical analyses were performed by Student's *t*-test. Bars indicate ± SE. *, $P < 0.05$; ***, $P < 0.001$. (g, n) Quantification of cell death by electrolyte leakage measurement. Means and SEs were calculated from three independent experiments. The statistical analyses were performed with Student's *t*-test. Bars indicate ± SE. *, $P < 0.05$; **, $P < 0.01$; ***, $P < 0.001$.

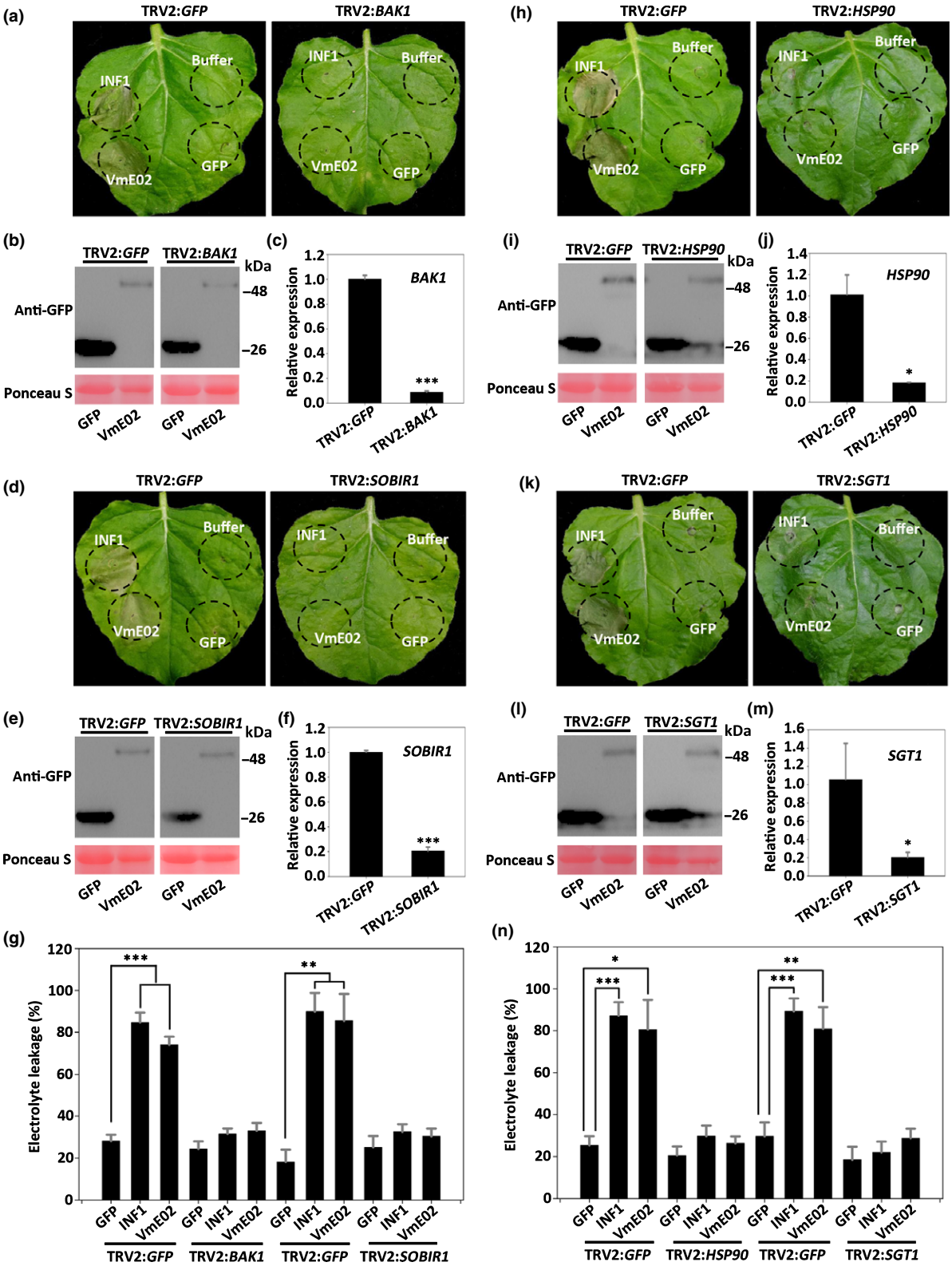

VmE02 affects conidiation of *V. mali*

To determine the biological role of VmE02 during *V. mali* infection, we first analyzed the expression profile of *VmE02* by qRT-PCR. It revealed that the transcript levels of *VmE02* were markedly induced at early stages of pathogen infection (6, 12 and 24 hpi), reaching a maximum at 6 hpi (Fig. S10). This indicates that *VmE02* is probably involved in *V. mali* infection of apple

host. To further investigate its potential virulence role, *VmE02* gene deletion mutants were generated. Positive transformants of target gene deletion were verified by PCR and Southern blotting analysis (Fig. S11a,b). All deletion mutants exhibited normal filamentous growth (Fig. S11c,d). Virulence tests showed that, compared with the wild-type strain 03-8, the deletion mutants △*VmE02*-5 and △*VmE02*-81 had no apparent influence on disease symptoms (Fig. S11e,f).

We next evaluated whether VmE02 influences conidiation of *V. mali*. Interestingly, after culturing on 20% apple bark agar medium for 45 d, the deletion mutants generated considerably reduced number of pycnidia, with △*VmE02*-5 decreased to 15.3% and △*VmE02*-81 decreased to 3.6%, compared with the wild-type strain 03-8 (Fig. 8a,b). Conversely, by introducing complementing plasmids into the deletion mutants (Fig. S12), their production of pycnidia recovered to comparable size with 03-8 (Fig. 8c,d). To further test whether VmE02 affects *V. mali* conidiation during its infection of host, we inoculated these strains on apple twigs. This illustrated that, 15 d post inoculation, the pycnidia production of both △*VmE02*-5 and △*VmE02*-81 were apparently reduced, compared with the wild-type strain (Fig. 8e,f). In contrast, the pycnidia number of *VmE02* complementation mutants was similar in size to that of 03-8 (Fig. 8e,f). These results suggest that *VmE02* positively regulates pathogen conidiation.

VmE02 enhances *N. benthamiana* resistance to fungal and oomycete pathogens

To investigate whether VmE02 modulates plant resistance against filamentous pathogens, the fungus *S. sclerotiorum* and the oomycete pathogen *P. capsici* were used to infect *N. benthamiana*. *N. benthamiana* leaves were infiltrated with 500 nM VmE02 purified protein 24 h before pathogen inoculation. We found that VmE02-treated leaves exhibited greatly enhanced resistance to *S. sclerotiorum* and *P. capsici*, compared with the control treated leaves (Fig. 9). These data suggest that VmE02 can boost *N. benthamiana* resistance to both fungal and oomycete pathogens.

Discussion

In plant–microbe systems, detection of PAMPs by plants results in PTI, which constitutes the front line of barrier against the majority of microbial invaders (Medzhitov, 2007; Boutrot & Zipfel, 2017). Nevertheless, our knowledge about the range of PAMPs is markedly little. Here, we identified a novel microbial PAMP, VmE02, that is conserved in filamentous pathogens.

VmE02 is a small cysteine-rich protein. It is possible that the cysteine residues of VmE02 form multiple disulfide bonds to stabilize VmE02 tertiary structure. This stabilization would, in turn, function to protect VmE02 against degradation by apoplastic plant proteases, as has been shown for other secreted apoplastic fungal proteins (Rep, 2005; Stergiopoulos & de Wit, 2009). Consistently, in this study, though VmE02 induced cell death with or without SP, full-length VmE02 activated earlier and stronger cell death than VmE02$^{\triangle SP}$ did (Fig. 2a–d), indicating the importance of extracellular space for VmE02 function. This finding is similar to the case of SsCP1, a cerato-platanin (CP) protein and cell death elicitor from *S. sclerotiorum* (Yang *et al.*, 2017). CPs are known as extracellular proteins, whereas, SsCP1 without SP also triggers cell death that is less severe than full-length SsCP1 does (Yang *et al.*, 2017). For validation of the apoplastic location of VmE02, we showed that full-length VmE02, but not VmE02$^{\triangle SP}$, can be detected in apoplast of *N. benthamiana* cells, by both protein detection from apoplastic fluid and GFP fluorescence labeling (Figs 2f, S5). Moveover, one homologue of VmE02 from *C. fulvum*, Ecp54-1 (A0A1P8YXP7, Fig. 2), was identified in apoplastic fluid of *C. fulvum*-infected tomato leaves (Mesarich *et al.*, 2018), further supporting the apoplast location for the function of VmE02.

In this study, VmE02 was shown to be widely spread in filamentous pathogens, and homologues of VmE02 exhibit high similarity at sequence level (Figs S6, S7). In addition, oomycete and fungal species contain VmE02 homologues that are also capable of trigging cell death in *N. benthamiana* (Fig. 4), suggesting a conserved role in cell death activation of these proteins. However, not all VmE02 homologues exhibited cell death phenotype when transiently expressed in *N. benthamiana* (Fig. 4). There are several possible explanations for this finding. One is that the homologues failed to trigger cell death because they may lack the surface-exposed epitope(s) required for perception by as yet unknown PRRs in *N. benthamiana* that recognize VmE02. Another explanation is that these proteins might possess divergent functions, which could be supported by a few lines of evidence. First, the number of VmE02 homologues varies in different species (Fig. 3b), and the sequence of these proteins shows various diversification, especially those in the biotrophic rust fungi (Fig. S7). VmE02 homologues in rust fungi are much more abundant than those in other species (Fig. 3b), and their sequences are variously extended at the N-terminus (Fig. S7). Second, cell death confers an evolutionary disadvantage to some certain organisms, especially biotrophs and hemibiotrophs that derive nutrients from living plant cells. Third, this finding is reminiscent of two other cell-death-inducing protein families, NLPs and CPs, which have been shown to diversify in function (Dong *et al.*, 2012; Santhanam *et al.*, 2013; Baccelli, 2015). Only two out of seven in *Verticillium dahliae* and seven out of 19 NLPs from *Phytophthora sojae* could induce plant cell death (Dong *et al.*, 2012; Santhanam *et al.*, 2013); the CP protein SP1 from *Leptosphaeria maculans* and MSP1 from *Magnaporthe grisea* failed to induce tissue necrosis, in contrast to the elicitor activity of most CPs (Wilson *et al.*, 2002; Jeong *et al.*, 2007).

We showed in this study that VmE02 activated innate immunity responses in *N. benthamiana*, including ROS burst, callose deposition, upregulation of HR-specific marker genes, and activation of SA- and JA-mediated resistance pathways (Figs 5, S8). This led us to speculate VmE02 to be a potential PAMP. Consistent with our hypothesis, VmE02 dramatically activated the expression of PTI-marker genes (Fig. 6). Most importantly, two LRR-RLKs, BAK1 and SOBIR1, were shown to be indispensable for VmE02-triggered cell death in *N. benthamiana* (Fig. 7a–g),

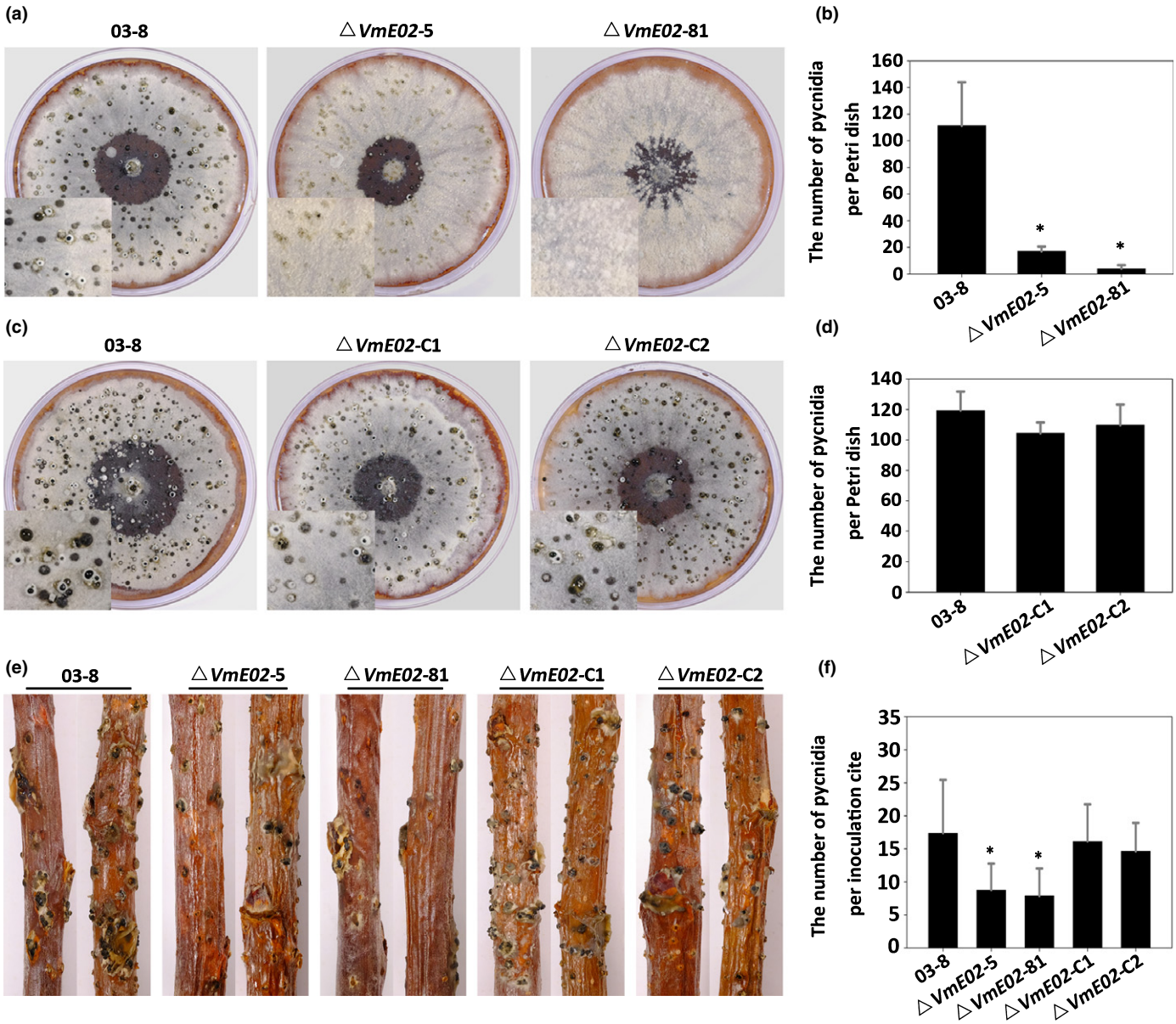

Fig. 8 Knocking out *VmE02* in *Valsa mali* attenuates pathogen conidiation. (a, c) Phenotype of pycnidia production by the wild-type strain 03-8, *VmE02*-deletion mutants (△*VmE02*-5 and △*VmE02*-81), and *VmE02*-complementation transformants (△*VmE02*-C1 and △*VmE02*-C2) on Petri dishes. (b, d) Quantification of pycnidia on 03-8, △*VmE02*-5, △*VmE02*-81, △*VmE02*-C1 and △*VmE02*-C2 cultured media. Wild-type strain 03-8, *VmE02*-deletion mutants and *VmE02*-complementation mutants were grown on 20% apple bark agar medium for 45 d at 25°C. Representative photographs for pycnidia production are shown. (e) Phenotype of pycnidia production by wild-type strain 03-8, *VmE02*-deletion mutants, and *VmE02*-complementation transformants in detached apple twigs. *V. mali* strains were inoculated on detached apple (*Malus domestica* Borkh. cv Fuji) twigs and maintained in a chamber room at 25°C. Photographs were taken 15 d post inoculation. (f) Quantification of pycnidia produced by wild-type strain 03-8, *VmE02*-deletion mutants, and *VmE02*-complementation transformants in detached apple twigs. The experiment was performed three times with similar results. Each assay was performed on six independent biological repeats. The statistical analyses were conducted by Student's *t*-test. Bars indicate ± SE. *, $P < 0.05$.

further confirming VmE02 to be a PAMP. We also showed that infiltration of VmE02 in *N. benthamiana* conferred plant resistance to both fungal and oomycete pathogens (Fig. 9), which is probably attributable to the recognition of VmE02 by PRR(s) and the subsequent plant defense responses. Apart from BAK1 and SOBIR1, we found that VmE02-induced cell death requires HSP90 and SGT1, two intracellular components known for R protein-mediated resistance signaling (Fig. 7h–n). HSP90 and SGT1 are known to form the structurally conserved HSP90-SGT1 complex, which is functionally conserved in sensing R proteins (Shirasu, 2009). However, the observation that both HSP90 and SGT1 are indispensable for VmE02-triggered cell death reflects that they also mediate recognition of extracellular molecules. This is similar to the case of INF1 elicitin, which also depends on HSP90 and SGT1 for cell death activation (Peart *et al.*, 2002; Kanzaki *et al.*, 2003). It has been explained that multiple resistance pathways might be convergently or parallelly affected by SGT1 (Peart *et al.*, 2002). Taken from all these

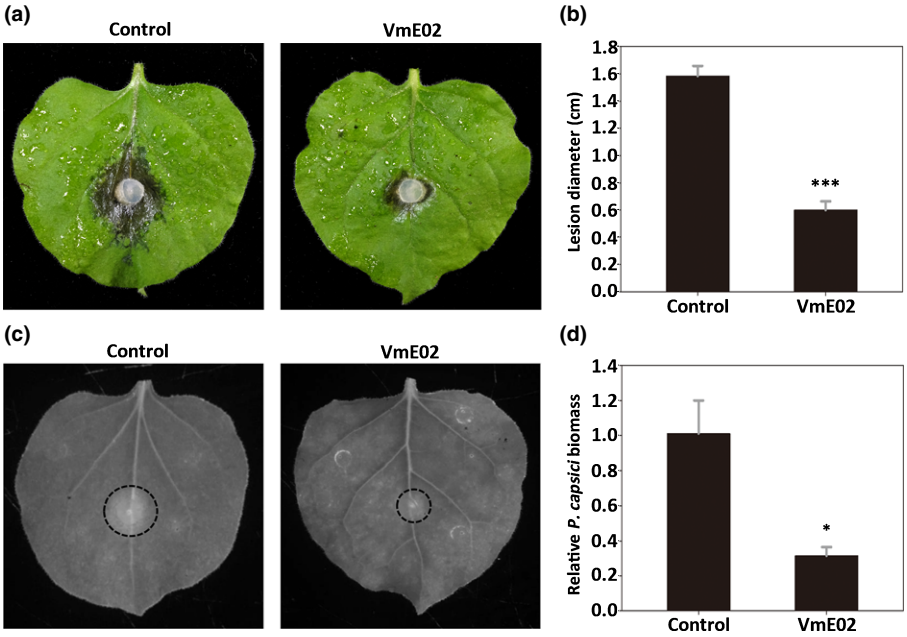

Fig. 9 VmE02 enhances *Nicotiana benthamiana* resistance to *Sclerotinia sclerotiorum* and *Phytophthora capsici*. *N. benthamiana* leaves were infiltrated with 500 nM purified VmE02 protein or buffer control separately 24 h before pathogen inoculation. (a) Symptom of *N. benthamiana* leaves 24 h post inoculation of *S. sclerotiorum*. (b) Diameters of lesions on *N. benthamiana* leaves infected by *S. sclerotiorum*. (c) Symptom of *N. benthamiana* leaves 60 h post inoculation of *P. capsici*. (d) Quantification of *P. capsici* infection by quantitative reverse transcription PCR analysis to measure the ratios of *P. capsici* to *N. benthamiana* DNA. The experiment was performed three times with similar results. Means and SEs were calculated from three biological replicates. The statistical analyses were performed with Student's *t*-test. Bars indicate ± SE. *, $P < 0.05$; ***, $P < 0.001$.

findings, it may be the same for HSP90, or probably the HSP90-SGT1 complex.

In order to explore the biological function of VmE02, we knocked out *VmE02* in *V. mali.* Despite its upregulation during early stages of infection (Fig. S10), *VmE02* deletion mutants had no apparent effect on pathogen virulence (Fig. S11e,f). This observation indicates that VmE02 may not function as a virulence effector during *V. mali* infection, which is in contrast to NLPs and CPs, proteins being both PAMPs and effectors (Böhm *et al.*, 2014; Pazzagli *et al.*, 2014). On the other hand, we cannot exclude the possibility that *VmE02* is functionally redundant in virulence, a phenomenon that is common for secreted proteins of filamentous pathogens (Win *et al.*, 2012). For example, gene disruption of 78 predicted effector genes from *Magnaporthe oryzae* showed that only one exhibited reduced virulence on rice (Saitoh *et al.*, 2012). Additionally, individual deletion of effector gene clusters in *Ustilago maydis* showed modest influence on virulence; however, these effector gene clusters make an additive contribution to virulence (Brefort *et al.*, 2014). Albeit with its marginal influence on virulence, however, VmE02 was found to severely influence conidiation of *V. mali* (Fig. 8). This is consistent with many other PAMPs that are essential for the normal life cycle of microbes (Medzhitov & Janeway, 1997; Nürnberger & Brunner, 2002; Thomma *et al.*, 2011). In addition, it may represent an explanation as to why VmE02 is retained in filamentous pathogens, regardless of its perception by plants.

Conserved molecules of pathogens generally play essential roles in microbial evolution, for which they can sometimes be acquired by other species through HGT, which allows the movement of genetic material between different organisms (Keeling & Palmer, 2008). For example, the *V. dahliae* effector Ave1, which exists in multiple phytopathogenic fungi and bacteria, was shown to be transferred from plants to *V. dahliae* but in turn markedly promotes fungal virulence (de Jonge *et al.*, 2012). Moreover, horizontal transfer of the interspecies-conserved effector gene *ToxA* from *Stagonospora nodorum* to *Pyrenophora tritici-repentis* resulted in emergence of the new tan spot disease in wheat fields (Friesen *et al.*, 2006). Here, VmE02 is a PAMP horizontally transferred from fungi to *Phytophthora* species (Fig. 2a). Actually, HGT can frequently occur between fungal and oomycete species (Richards *et al.*, 2011; Soanes & Richards, 2014). For example, 34 gene families, including transporters, secreted enzymes and NLPs, were horizontally transferred between fungi and oomycetes, which may facilitate the parasitic evolution of oomycetes (Richards *et al.*, 2011). Moreover, according to the phylogenetic analysis of the *P. sojae* XEG1 (Ma *et al.*, 2015), this PAMP is probably derived from fungal species as well. It would be of interest to investigate the function of VmE02 homologues in its recipient species.

In conclusion, our results revealed a novel cross-kingdom PAMP in filamentous pathogens. To explain how VmE02 is perceived by plants and activates plant immunity, future studies will be focused on exploration of receptors or signaling components targeted by VmE02.

Acknowledgements

We thank Professor Jinrong Xu at Northwest A&F University for providing the pDL2-*GFP* plasmids and Professor Qing Ma at Northwest A&F University for providing the TRV plasmids. This work was supported by the National Natural Science Foundation of China (nos. 31471732 and 31671982).

Author contributions

LH, JN, and ZY designed and conceived the research. JN, ZY and ZL performed the experiments. JN, ZY and LH analyzed the

data. JN, ZY and LH wrote the manuscript. YW contributed to discussion and revision. All authors discussed the results and commented on the manuscript.

ORCID

Jiajun Nie https://orcid.org/0000-0002-5765-0931
Yuxing Wu https://orcid.org/0000-0001-5118-9964
Zhiyuan Yin https://orcid.org/0000-0002-7189-895X

References

Albert I, Böhm H, Albert M, Feiler CE, Imkampe J, Wallmeroth N, Brancato C, Raaymakers TM, Oome S, Zhang H *et al.* 2015. An RLP23–SOBIR1–BAK1 complex mediates NLP-triggered immunity. *Nature Plants* **1**: e15140.

Asai S, Yoshioka H. 2009. Nitric oxide as a partner of reactive oxygen species participates in disease resistance to necrotrophic pathogen *Botrytis cinerea* in *Nicotiana benthamiana*. *Molecular Plant–Microbe Interactions* **22**: 619–629.

Baccelli I. 2015. Cerato-platanin family proteins: one function for multiple biological roles? *Frontiers in Plant Science* **5**: 2013–2016.

Bailey TL, Boden M, Buske FA, Frith M, Grant CE, Clementi L, Ren J, Li WW, Noble WS. 2009. MEME Suite: tools for motif discovery and searching. *Nucleic Acids Research* **37**: 202–208.

Böhm H, Albert I, Oome S, Raaymakers TM, Van den Ackerveken G, Nürnberger T. 2014. A conserved peptide pattern from a widespread microbial virulence factor triggers pattern-induced immunity in *Arabidopsis*. *PLoS Pathogens* **10**: e1004491.

Boutrot F, Zipfel C. 2017. Function, discovery, and exploitation of plant pattern recognition receptors for broad-spectrum disease resistance. *Annual Review of Phytopathology* **55**: 257–286.

Brefort T, Tanaka S, Neidig N, Doehlemann G, Vincon V, Kahmann R. 2014. Characterization of the largest effector gene cluster of *Ustilago maydis*. *PLoS Pathogens* **10**: e1003866.

Brunner F, Rosahl S, Lee J, Rudd JJ, Geiler C, Kauppinen S, Rasmussen G, Scheel D, Nürnberger T. 2002. Pep-13, a plant defense-inducing pathogen-associated pattern from *Phytophthora* transglutaminases. *EMBO Journal* **21**: 6681–6688.

Chinchilla D, Zipfel C, Robatzek S, Kemmerling B, Nürnberger T, Jones JDG, Felix G, Boller T. 2007. A flagellin-induced complex of the receptor FLS2 and BAK1 initiates plant defence. *Nature* **448**: 497–500.

Coll NS, Epple P, Dangl JL. 2011. Programmed cell death in the plant immune system. *Cell Death and Differentiation* **18**: 1247–1256.

Dean JD, Goodwin PH, Hsiang T. 2005. Induction of glutathione *S*-transferase genes of *Nicotiana benthamiana* following infection by *Colletotrichum destructivum* and *C. orbiculare* and involvement of one in resistance. *Journal of Experimental Botany* **56**: 1525–1533.

Dong S, Kong G, Qutob D, Yu X, Tang J, Kang J, Dai T, Wang H, Gijzen M, Wang Y. 2012. The NLP toxin family in *Phytophthora sojae* includes rapidly evolving groups that lack necrosis-inducing activity. *Molecular Plant–Microbe Interactions* **25**: 896–909.

Dow M, Newman M, Von Roepenack E. 2000. The induction and modulation of plant defense responses by bacterial lipopolysaccharides. *Annual Review of Microbiology* **38**: 241–261.

Du J, Verzaux E, Chaparro-Garcia A, Bijsterbosch G, Keizer LCP, Zhou J, Liebrand TWH, Xie C, Govers F, Robatzek S *et al.* 2015. Elicitin recognition confers enhanced resistance to *Phytophthora infestans* in potato. *Nature Plants* **1**: e15034.

Edgar RC. 2004. MUSCLE: multiple sequence alignment with high accuracy and high throughput. *Nucleic Acids Research* **32**: 1792–1797.

Felix G, Boller T. 2003. Molecular sensing of bacteria in plants: the highly conserved RNA-binding motif RNP-1 of bacterial cold shock proteins is recognized as an elicitor signal in tobacco. *Journal of Biological Chemistry* **278**: 6201–6208.

Felix G, Duran JD, Volko S, Boller T. 1999. Plants have a sensitive perception system for the most conserved domain of bacterial flagellin. *The Plant Journal* **18**: 265–276.

Fliegmann J, Mithöfer A, Wanner G, Ebel J. 2004. An ancient enzyme domain hidden in the putative β-glucan elicitor receptor of soybean may play an active part in the perception of pathogen-associated molecular patterns during broad host resistance. *Journal of Biological Chemistry* **279**: 1132–1140.

Fradin EF, Zhang Z, Juarez Ayala JC, Castroverde CDM, Nazar RN, Robb J, Liu C-M, Thomma BPHJ. 2009. Genetic dissection of *Verticillium* wilt resistance mediated by tomato *Ve1*. *Plant Physiology* **150**: 320–332.

Franco-Orozco B, Berepiki A, Ruiz O, Gamble L, Griffe LL, Wang S, Birch PRJ, Kanyuka K, Avrova A. 2017. A new proteinaceous pathogen-associated molecular pattern (PAMP) identified in ascomycete fungi induces cell death in Solanaceae. *New Phytologist* **214**: 1657–1672.

Friesen TL, Stukenbrock EH, Liu Z, Meinhardt S, Ling H, Faris JD, Rasmussen JB, Solomon PS, McDonald BA, Oliver RP. 2006. Emergence of a new disease as a result of interspecific virulence gene transfer. *Nature Genetics* **38**: 953–956.

Gao J, Li Y, Ke X, Kang Z, Huang L. 2011. Development of genetic transformation system of *Valsa mali* of apple mediated by PEG. *Acta Microbiologica Sinica* **51**: 1194–1199.

Gust AA, Biswas R, Lenz HD, Rauhut T, Ranf S, Kemmerling B, Götz F, Glawischnig E, Lee J, Felix G *et al.* 2007. Bacteria-derived peptidoglycans constitute pathogen-associated molecular patterns triggering innate immunity in *Arabidopsis*. *Journal of Biological Chemistry* **282**: 32338–32348.

Gust AA, Felix G. 2014. Receptor like proteins associate with SOBIR1-type of adaptors to form bimolecular receptor kinases. *Current Opinion in Plant Biology* **21**: 104–111.

Hajdukiewicz P, Svab Z, Maliga P. 1994. The small, versatile *pPZP* family of *Agrobacterium* binary vectors for plant transformation. *Plant Molecular Biology* **25**: 989–994.

He Z, Zhang H, Gao S, Lercher MJ, Chen WH, Hu S. 2016. EVOLVIEW v2: an online visualization and management tool for customized and annotated phylogenetic trees. *Nucleic Acids Research* **44**: W236–W241.

Heese A, Hann DR, Gimenez-Ibanez S, Jones AME, He K, Li J, Schroeder JI, Peck SC, Rathjen JP. 2007. The receptor-like kinase SERK3/BAK1 is a central regulator of innate immunity in plants. *Proceedings of the National Academy of Sciences, USA* **104**: 12217–12222.

Imai R, Koike M, Sutoh K, Kawakami A, Torada A, Oono K. 2005. Molecular characterization of a cold-induced plasma membrane protein gene from wheat. *Molecular Genetics and Genomics* **274**: 445–453.

Jacobs KA, Collins-Racie LA, Colbert M, Duckett M, Golden-Fleet M, Kelleher K, Kriz R, La Vallie ER, Merberg D, Spaulding V *et al.* 1997. A genetic selection for isolating cDNAs encoding secreted proteins. *Gene* **198**: 289–296.

Jehle AK, Lipschis M, Albert M, Fallahzadeh-Mamaghani V, Furst U, Mueller K, Felix G. 2013. The receptor-like protein ReMAX of *Arabidopsis* detects the microbe-associated molecular pattern eMax from *Xanthomonas*. *Plant Cell* **25**: 2330–2340.

Jeong JS, Mitchell TK, Dean RA. 2007. The *Magnaporthe grisea* snodprot1 homolog, MSP1, is required for virulence. *FEMS Microbiology Letters* **273**: 157–165.

de Jonge R, van Esse HP, Maruthachalam K, Bolton MD, Santhanam P, Saber MK, Zhang Z, Usami T, Lievens B, Subbarao KV *et al.* 2012. Tomato immune receptor Ve1 recognizes effector of multiple fungal pathogens uncovered by genome and RNA sequencing. *Proceedings of the National Academy of Sciences, USA* **109**: 5110–5115.

Kanneganti T, Huitema E, Cakir C, Kamoun S. 2006. Synergistic interactions of the plant cell death pathways induced by *Phytophthora infestans* Nep1-like protein PiNPP1.1 and INF1 elicitin. *Molecular Plant–Microbe Interactions* **19**: 854–863.

Kanzaki H, Saitoh H, Ito A, Fujisawa S, Kamoun S, Katou S, Yoshioka H, Terauchi R. 2003. Cytosolic HSP90 and HSP70 are essential components of INF1-mediated hypersensitive response and non-host resistance to *Pseudomonas cichorii* in *Nicotiana benthamiana*. *Molecular Plant Pathology* **4**: 383–391.

Ke X, Huang L, Han Q, Gao X, Kang Z. 2013. Histological and cytological investigations of the infection and colonization of apple bark by *Valsa mali* var. *mali*. *Australasian Plant Pathology* **42**: 85–93.

Keeling PJ, Palmer JD. 2008. Horizontal gene transfer in eukaryotic evolution. *Nature Reviews Genetics* **9**: 605–618.

Kumar S, Stecher G, Tamura K. 2016. MEGA7: molecular evolutionary genetics analysis version 7.0 for bigger datasets. *Molecular Biology and Evolution* **33**: 1870–1874.

Li Z, Gao X, Du Z, Hu Y, Kang Z, Huang L. 2013. Survey of apple valsa canker in Weibei area of Shaanxi province. *Acta Agriculturae Boreali-Occidentalis Sinica* **1**: 029.

Li Z, Yin Z, Fan Y, Xu M, Kang Z, Huang L. 2015. Candidate effector proteins of the necrotrophic apple canker pathogen *Valsa mali* can suppress BAX-induced PCD. *Frontiers in Plant Science* **6**: 1–9.

Liang X, Zhou J. 2018. Receptor-like cytoplasmic kinases: central players in plant receptor kinase-mediated signaling. *Annual Review of Phytopathology* **69**: 267–299.

Liebrand TWH, van den Berg GCM, Zhang Z, Smit P, Cordewener JH, America AHP, Sklenar J, Jones AME, Tameling WIL, Robatzek S *et al.* 2013. Receptor-like kinase SOBIR1/EVR interacts with receptor-like proteins in plant immunity against fungal infection. *Proceedings of the National Academy of Sciences, USA* **110**: 10010–10015.

Liebrand TWH, van den Burg HA, Joosten MHAJ. 2014. Two for all: receptor-associated kinases SOBIR1 and BAK1. *Trends in Plant Science* **19**: 123–132.

Liu W, Xie Y, Ma J, Luo X, Nie P, Zuo Z, Lahrmann U, Zhao Q, Zheng Y, Zhao Y *et al.* 2015. IBS: an illustrator for the presentation and visualization of biological sequences. *Bioinformatics* **31**: 3359–3361.

Liu Y, Schiff M, Marathe R, Dinesh-Kumar SP. 2002. Tobacco *Rar1*, *EDS1* and *NPR1/NIM1* like genes are required for *N*-mediated resistance to tobacco mosaic virus. *The Plant Journal* **30**: 415–429.

Livak KJ, Schmittgen TD. 2001. Analysis of relative gene expression data using real-time quantitative PCR and the $2^{-\Delta\Delta CT}$ method. *Methods* **25**: 402–408.

Ma Z, Song T, Zhu L, Ye W, Wang Y, Shao Y, Dong S, Zhang Z, Dou D, Zheng X *et al.* 2015. A *Phytophthora sojae* glycoside hydrolase 12 protein is a major virulence factor during soybean infection and is recognized as a PAMP. *Plant Cell* **27**: 2057–2072.

McLellan H, Boevink PC, Armstrong MR, Pritchard L, Gomez S, Morales J, Whisson SC, Beynon JL, Birch PRJ. 2013. An RxLR effector from *Phytophthora infestans* prevents re-localisation of two plant NAC transcription factors from the endoplasmic reticulum to the nucleus. *PLoS Pathogens* **9**: e1003670.

Medzhitov R. 2007. Recognition of microorganisms and activation of the immune response. *Nature* **449**: 819–826.

Medzhitov R, Janeway CAJ. 1997. Innate immunity: the virtues of a nonclonal system of recognition. *Cell* **91**: 295–298.

Mesarich CH, Ökmen Bilal, Rovenich H, Griffiths SA, Wang C, Jashni MK, Mihajlovski A, Collemare J, Hunziker L, Deng CH *et al.* 2018. Specific hypersensitive response-associated recognition of new apoplastic effectors from *Cladosporium fulvum* in wild tomato. *Molecular Plant–Microbe Interactions* **31**: 145–162.

Nürnberger T, Brunner F. 2002. Innate immunity in plants and animals: emerging parallels between the recognition of general elicitors and pathogen-associated molecular patterns. *Current Opinion in Plant Biology* **5**: 318–324.

O'Leary BM, Rico A, McCraw S, Fones HN, Preston GM. 2014. The infiltration–centrifugation technique for extraction of apoplastic fluid from plant leaves using *Phaseolus vulgaris* as an example. *Journal of Visualized Experiments* **94**: 1–8.

Oome S, Raaymakers TM, Cabral A, Samwel S, Böhm H, Albert I, Nürnberger T, Van den Ackerveken G. 2014. Nep1-like proteins from three kingdoms of life act as a microbe-associated molecular pattern in *Arabidopsis*. *Proceedings of the National Academy of Sciences, USA* **111**: 16955–16960.

Pazzagli L, Seidl-Seiboth V, Barsottini M, Vargas WA, Scala A, Mukherjee PK. 2014. Cerato-platanins: elicitors and effectors. *Plant Science* **228**: 79–87.

Peart JR, Lu R, Sadanandom A, Malcuit I, Moffett P, Brice DC, Schauser L, Jaggard DAW, Xiao S, Coleman MJ *et al.* 2002. Ubiquitin ligase-associated protein SGT1 is required for host and nonhost disease resistance in plants. *Proceedings of the National Academy of Sciences, USA* **99**: 10865–10869.

Pieterse CMJ, Van der Does D, Zamioudis C, Leon-Reyes A, Van Wees SCM. 2012. Hormonal modulation of plant immunity. *Annual Review of Cell and Developmental Biology* **28**: 489–521.

Pontier D, Godiard L, Marco Y, Roby D. 1994. *hsr203J*, a tobacco gene whose activation is rapid, highly localized and specific for incompatible plant/pathogen interactions. *The Plant Journal* **5**: 507–521.

Qi M, Link TI, Müller M, Hirschburger D, Pudake RN, Pedley KF, Braun E, Voegele RT, Baum TJ, Whitham SA. 2016. A small cysteine-rich protein from the Asian soybean rust fungus, *Phakopsora pachyrhizi*, suppresses plant immunity. *PLoS Pathogens* **12**: 1–29.

Qutob D, Kemmerling B, Brunner F, Kufner I, Engelhardt S, Gust AA, Luberacki B, Seitz HU, Stahl D, Rauhut T *et al.* 2006. Phytotoxicity and innate immune responses induced by Nep1-like proteins. *Plant Cell* **18**: 3721–3744.

Rep M. 2005. Small proteins of plant-pathogenic fungi secreted during host colonization. *FEMS Microbiology Letters* **253**: 19–27.

Richards TA, Soanes DM, Jones MDM, Vasieva O, Leonard G, Paszkiewicz K, Foster PG, Hall N, Talbot NJ. 2011. Horizontal gene transfer facilitated the evolution of plant parasitic mechanisms in the oomycetes. *Proceedings of the National Academy of Sciences, USA* **108**: 15258–15263.

Rodriguez PA, Stam R, Warbroek T, Bos JIB. 2014. Mp10 and Mp42 from the aphid species *Myzus persicae* trigger plant defenses in *Nicotiana benthamiana* through different activities. *Molecular Plant–Microbe Interactions* **27**: 30–39.

Rotblat B, Enshell-Seijffers D, Gershoni JM, Schuster S, Avni A. 2002. Identification of an essential component of the elicitation active site of the EIX protein elicitor. *The Plant Journal* **32**: 1049–1055.

Sainsbury F, Lomonossoff GP. 2008. Extremely high-level and rapid transient protein production in plants without the use of viral replication. *Plant Physiology* **148**: 1212–1218.

Saitoh H, Fujisawa S, Mitsuoka C, Ito A, Hirabuchi A, Ikeda K, Irieda H, Yoshino K, Yoshida K, Matsumura H *et al.* 2012. Large-scale gene disruption in *Magnaporthe oryzae* identifies MC69, a secreted protein required for infection by monocot and dicot fungal pathogens. *PLoS Pathogens* **8**: e1002711.

Santhanam P, van Esse HP, Albert I, Faino L, Nürnberger T, Thomma BPHJ. 2013. Evidence for functional diversification within a fungal NEP1-like protein family. *Molecular Plant–Microbe Interactions* **278**: 278–286.

Shinya T, Nakagawa T, Kaku H, Shibuya N. 2015. Chitin-mediated plant–fungal interactions: catching, hiding and handshaking. *Current Opinion in Plant Biology* **26**: 64–71.

Shirasu K. 2009. The HSP90-SGT1 chaperone complex for NLR immune sensors. *Annual Review of Plant Biology* **60**: 139–164.

Soanes D, Richards TA. 2014. Horizontal gene transfer in eukaryotic plant pathogens. *Annual Review of Phytopathology* **52**: 583–614.

Stergiopoulos I, de Wit PJGM. 2009. Fungal effector proteins. *Annual Review of Phytopathology* **47**: 233–263.

Takahashi Y, Berberich T, Yamashita K, Uehara Y, Miyazaki A, Kusano T. 2004. Identification of tobacco *HIN1* and two closely related genes as spermine-responsive genes and their differential expression during the *Tobacco mosaic virus*-induced hypersensitive response and during leaf- and flower-senescence. *Plant Molecular Biology* **54**: 613–622.

Thomma BPHJ, Nürnberger T, Joosten MHAJ. 2011. Of PAMPs and effectors: the blurred PTI–ETI dichotomy. *Plant Cell* **23**: 4–15.

Voinnet O, Rivas S, Mestre P, Baulcombe D. 2003. An enhanced transient expression system in plants based on suppression of gene silencing by the p19 protein of tomato bushy stunt virus. *The Plant Journal* **33**: 949–956.

Wagner B, Fuchs H, Adhami F, Ma Y, Scheiner O, Breiteneder H. 2004. Plant virus expression systems for transient production of recombinant allergens in *Nicotiana benthamiana*. *Methods* **32**: 227–234.

Wang Y, Xu Y, Sun Y, Wang H, Qi J, Wan B, Ye W, Lin Y, Shao Y, Dong S *et al.* 2018. Leucine-rich repeat receptor-like gene screen reveals that *Nicotiana* RXEG1 regulates glycoside hydrolase 12 MAMP detection. *Nature Communications* **9**: e594.

Wei J, Huang L, Gao Z, Ke X, Kang Z. 2010. Laboratory evaluation methods of apple *Valsa* canker disease caused by *Valsa ceratosperma sensu* Kobayashi. *Acta Phytopathologica Sinica* **40**: 14–20.

Wilson LM, Idnurm A, Howlett BJ. 2002. Characterization of a gene (sp1) encoding a secreted protein from *Leptosphaeria maculans*, the blackleg pathogen of *Brassica napus*. *Molecular Plant Pathology* **3**: 487–493.

Win J, Chaparro-Garcia A, Belhaj K, Saunders DGO, Yoshida K, Dong S, Schornack S, Zipfel C, Robatzek S, Hogenhout SA *et al.* 2012. Effector

biology of plant-associated organisms: concepts and perspectives. *Cold Spring Harbor Symposia on Quantitative Biology* 77: 235–247.

Yang G, Tang L, Gong Y, Xie J, Fu Y, Jiang D, Li G, Collinge DB, Chen W, Cheng J. 2017. A cerato-platanin protein SsCP1 targets plant PR1 and contributes to virulence of *Sclerotinia sclerotiorum*. *New Phytologist* **217**: 739–755.

Yasuda S, Okada K, Saijo Y. 2017. A look at plant immunity through the window of the multitasking coreceptor BAK1. *Current Opinion in Plant Biology* **38**: 10–18.

Yin Z, Ke X, Huang D, Gao X, Voegele RT, Kang Z, Huang L. 2013. Validation of reference genes for gene expression analysis in *Valsa mali* var. *mali* using real-time quantitative PCR. *World Journal of Microbiology and Biotechnology* **29**: 1563–1571.

Yin Z, Liu H, Li Z, Ke X, Dou D, Gao X, Song N, Dai Q, Wu Y, Xu JR *et al.* 2015. Genome sequence of *Valsa* canker pathogens uncovers a potential adaptation of colonization of woody bark. *New Phytologist* **208**: 1202–1216.

Yin Z, Zhu B, Feng H, Huang L. 2016. Horizontal gene transfer drives adaptive colonization of apple trees by the fungal pathogen *Valsa mali*. *Scientific Reports* **6**: 33129.

Yu X, Feng B, He P, Shan L. 2017. From chaos to harmony: responses and signaling upon microbial pattern recognition. *Annual Review of Phytopathology* **55**: 109–137.

Yu X, Tang J, Wang Q, Ye W, Tao K, Duan S, Lu C, Yang X, Dong S, Zheng X *et al.* 2012. The RxLR effector Avh241 from *Phytophthora sojae* requires plasma membrane localization to induce plant cell death. *New Phytologist* **196**: 247–260.

Zhang L, Kars I, Essenstam B, Liebrand TWH, Wagemakers L, Elberse J, Tagkalaki P, Tjoitang D, van den Ackerveken G, van Kan JAL. 2014. Fungal endopolygalacturonases are recognized as microbe-associated molecular patterns by the *Arabidopsis* receptor-like protein RESPONSIVENESS TO BOTRYTIS POLYGALACTURONASES1. *Plant Physiology* **164**: 352–364.

Zhou X, Li G, Xu JR. 2011. Efficient approaches for generating GFP fusion and epitope-tagging constructs in filamentous fungi. *Methods in Molecular Biology* **722**: 199–212.

Supporting Information

Additional Supporting Information may be found online in the Supporting Information section at the end of the article:

Fig. S1 Targeted gene replacement strategy of G418-resistant cassette.

Fig. S2 Purified VmE02 recombinant protein produced by *Escherichia coli* exhibits cell death-inducing activity in *Nicotiana benthamiana* and tomato.

Fig. S3 The signal peptide (SP) of VmE02 is functional.

Fig. S4 GFP fused with N-terminal signal peptides cannot trigger cell death in *Nicotiana benthamiana*.

Fig. S5 Subcellular localization of VmE02 and VmE02$^{\Delta SP}$ in *Nicotiana benthamiana* epidermal cells.

Fig. S6 Conserved motifs of VmE02 and its homologs predicted by MEME suite.

Fig. S7 Amino acid sequence alignment of VmE02 and its homologous sequences.

Fig. S8 VmE02 actives the expression of defense-related genes in apple host.

Fig. S9 EDS1 and NDR1 are not required for VmE02-triggered cell death in *Nicotiana benthamiana*.

Fig. S10 Relative expression levels of *VmE02* at 0, 6, 12, 24, 36, and 48 h post inoculation of *Valsa mali* wild type strain 03-8 on apple twigs.

Fig. S11 *VmE02* gene deletion mutants are normal in filamentous growth and fully virulent on apple twigs.

Fig. S12 Western blotting analysis of proteins isolated from *VmE02* gene-complementation transformants.

Table S1 Primers used in this study.

Table S2 Candidate effector proteins of *Valsa mali*.

Please note: Wiley Blackwell are not responsible for the content or functionality of any Supporting Information supplied by the authors. Any queries (other than missing material) should be directed to the *New Phytologist* Central Office.